Multi-GeV Plasma Wakefield Acceleration Experiments

=

The E-168 Collaboration:

M. Berry, I. Blumenfeld, F.-J. Decker, M. J. Hogan*, N. Kirby, R. Ischebeck,
R. H. Iverson, R. H. Siemann and D. Walz
Stanford Linear Accelerator Center
C. E. Clayton, C. Huang, C. Joshi*, W. Lu, K. A. Marsh, W. B. Mori and M. Zhou
University of California, Los Angeles
T. Katsouleas, P. Muggli*, and X. Wang
University of Southern California

November 8, 2006

1 Abstract

In the past seven years plasma wakefield accelerators have emerged as a leading advanced accelerator scheme due to progress on a number of fronts (see [1]). The SLAC/UCLA/USC E-162/164/167 collaboration has been arguably the lead group pioneering this research. Accomplishments include the first demonstration that controlled beam propagation and high-gradient acceleration could be extended from the mm scale to meter scales (E-157 and E-162), the first acceleration of positrons (E-162) in a plasma, the first acceleration of electrons by more than one GeV (E-164X) and most recently doubling the energy of some of the electrons from 42 to 85 GeV in just 85cm (E-167). These experiments have yielded a number of rich new beam and plasma physics results, demonstrated the promise of beam-driven plasma accelerators and developed a sophisticated laboratory infrastructure for beam and plasma experiments in the Final Focus Test Beam (FFTB). The FFTB was decommissioned in April 2006 to make way for the Linac Coherent Light Source (LCLS). For the experiments proposed here we will relocate much of this infrastructure to the South Arc Beamline Experimental Region (SABER).

This proposal aims to explore the physics questions beyond energy doubling: What is the maximum energy gain achievable – can the energy be more than doubled? How much of the beam energy can be transferred to the plasma wake? Do instabilities become important over long plasma lengths and in the presence of large energy loss? Additionally, the >30GeV/m accelerating gradients demonstrated in E-164X and E-167 revealed a new physical phenomena where plasma electrons are trapped in the plasma wake and exit the plasma. Initial measurements hint that these self-injected particles have many intriguing features making them potentially interesting in their own right: pulse durations of 10's of fs and an emittance smaller than the bunch producing the plasma wake. Simulations indicate however that under certain conditions these trapped particles may load the accelerating wake, limit the energy transfer to the trailing bunch and reduce the overall plasma accelerator efficiency. Studying the trapping mechanism and the resulting bunch properties will be an integral part of our work.

These experiments are based largely on existing apparatus and on the experimental techniques developed over the years in the FFTB. During the commissioning phase of SABER, we will implement new and improved diagnostics (see Section 3.3) that will allow for a better measurement of the beam current distribution to further our understanding the processes in the plasma. Although it is expected to deliver a beam with peak current and transverse size similar to what was available in the FFTB, the proposed beam transport system at SABER will lead to significant emittance growth. We will thus expand and upgrade our optical transition radiation (OTR) monitors to allow for single shot, non-destructive emittance measurements and to aid beamline set-up and commissioning. Once beam parameters similar to those used in the FFTB will be established in SABER and our experimental apparatus will be relocated, our program will begin in earnest.

We anticipate this proposal will be the first in a series, beginning a second chapter of a long-term program studying beam-plasma interactions at SLAC. Future proposals will aim to exploit the upgraded capabilities proposed for the SABER completed facility – operational independence from LCLS and for the first time, compressed positrons.

2 Introduction

Motivation

During the last century, particle accelerators have steadily increased their energy, leading to extraordinary discoveries about the structure of the universe and finding their way into many practical applications from television tubes to medical diagnostics and treatment. The maximum particle energy has increased exponentially, increasing by a factor of 10 every decade.

However, the growth in electron/positron accelerator energy seems to have begun to level off in the last decades. This has been attributed to the fact that the technology of accelerating these particles with radiofrequency cavities is approaching its limits [2]. Various technologies have been proposed to extend the energy reach of these particle accelerators. Some extend existing RF technologies to higher frequencies or use dielectrics. However, they are all limited by breakdown on the material surface. This could be overcome by using a plasma as the accelerating medium, where the limit is several orders of magnitude larger.

The Plasma Wakefield Accelerator

Investigating the acceleration of particles and beams to very high energy in large gradient plasma modules therefore offers great potentials for future accelerators. In particular, the beam-driven or plasma wakefield accelerator (PWFA) scheme proposed by Fainberg et al. [3] could be used to double the energy of a future linear collider [4]. The basic concept of the plasma wakefield accelerator involves the passage of an ultra-relativistic electron bunch through a stationary plasma [5]. The plasma can be formed by ionizing a gas with a laser (as done in experiments E-157 and E-162), or through field-ionization by the Coulomb field of the relativistic bunch (experiments E-164, E-164X and E-167) [6]. This second method allows for the meter-long, dense (10^{16}-10^{17} cm^{-3}) plasmas suitable for the PWFA to be produced and greatly simplifies the experimental set-up. The head of the bunch creates the plasma and drives the wake, while the particles in the back witness the resulting high-gradient acceleration (see Figure 2). The system effectively operates as a transformer, where the energy from the particles in the head is transferred to those in the back through the plasma wake.

PWFA Principle

We begin by defining the symbols used throughout this proposal.

Table 1: Legend of symbols used in this proposal

Physical Parameter	Symbol
Speed of Light in Vacuum	c
Charge of an Electron	e
Classical Electron Radius	$e^2/4\pi\varepsilon_0 m_e c^2$
Accelerating Gradient	eE
Plasma Focusing Gradient	$K=\omega_p/(2\gamma)^{1/2}c$
Plasma Wavenumber	$k_p=\omega_p/c$
Plasma Wavelength	$\lambda_p=2\pi/k_p$
Mass of an Electron	m_e
Number of electrons per Bunch	N
Drive Beam Density	$n_b=N/(2\pi)^{3/2}\sigma^2_r\sigma_z$
Plasma Density	n_p
Drive Beam Transverse Size	σ_r
Drive Beam Bunch Length	σ_z
Beam Plasma Frequency	$\omega_{pb}=(n_b e^2/\varepsilon_o m_e)$
Electron Plasma Frequency	$\omega_p=(n_o e^2/\varepsilon_o m_e)$
Beta Function of the Beam	β
Normalized Emittance of the Beam	$\varepsilon_N=\gamma\varepsilon$
Spot Size of the Beam in x, y	σ_x, σ_y
Focal Length of the Lens in x, y	f_x, f_y
Skin Depth of Plasma	c/ω_p

In the beam-driven plasma wakefield accelerator (PWFA), a short but high current electron bunch, with beam density n_b larger than the plasma electron density n_p, expels the plasma electrons as shown in Figure 1. The expelled plasma electrons rush back in and set-up a large plasma wakefield which has a phase velocity equal to the beam velocity (≅ c). There are several accelerating buckets in the wakefield trailing the initial driving bunch. Ideally, one would place a witness bunch to be accelerated in one of these buckets. Appropriate techniques to craft two bunches spaced in time by roughly one plasma period are still being developed, however there is a key question that can be addressed with a single bunch – what is the magnitude of the accelerating field?

According to linear plasma theory the wake amplitude is [7]

$$eE_{linear}[eV/cm] = \sqrt{n_p}\,\frac{n_b}{n_p}\,\frac{\sqrt{2\pi}k_p^2\sigma_z^{\,2}e^{-\frac{k_p^2\sigma_z^2}{2}}}{1+\frac{1}{k_p^2\sigma_r^2}} \qquad (1)$$

For small transverse beam sizes ($k_p\sigma_r << 1$), the accelerating field is maximized for $k_p\sigma_z \approx \sqrt{2}$, i.e., when the plasma electrons rush back on axis immediately behind the bunch, and the accelerating field has a value given by

$$eE_{linear} = 240\,MeV/m\left(\frac{N}{4\times10^{10}}\right)\left(\frac{0.6}{\sigma_z(mm)}\right)^2 \qquad (2)$$

where N is the number of particles in the electron bunch and σ_z is the bunch length.

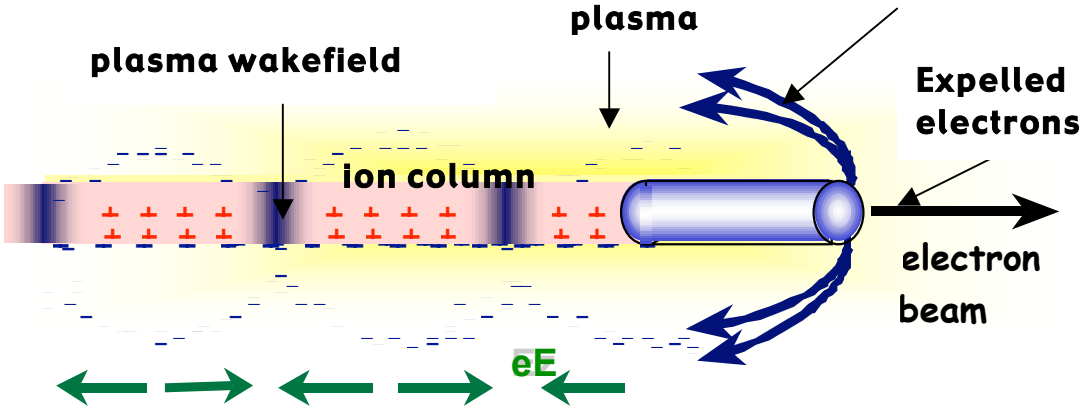

Figure 1: Physical mechanism of the Plasma Wakefield Accelerator.

When the wake is excited in this so called blow-out regime ($n_b > n_p$ and $k_p\sigma_r << 1$), the wake excitation is highly nonlinear (spikey) and can reach a higher peak value $(eE)_{peak}$ which can be three to four times $(eE)_{linear}$. For the portion of the wake that can be used as an accelerator, the amplitude is somewhere in between the peak value and the absolute value given by linear theory $(eE)_{linear}$.

The ion column left behind the head of the bunch also provides a very large focusing force (strength ≈ 3MT/m for $n_p=10^{17}$ cm^{-3}), which allows for the beam to drive the wake over many of its beta-functions. The combination of large focusing and accelerating gradient leads to the large energy gains observed in previous experiments.

Experiments E-164X and E-167 operated in new hybrid regime of PWFA where σ_r/σ_z is no longer << 1 and where $k_p\sigma_r \sim 1$ (recall $k_p = \sqrt{2}/\sigma_z$). In this case $n_b/n_0 \geq 1$ and the wakefield is weakly non-linear. Nevertheless, these experiments have

demonstrated the dramatic increase in accelerating gradients predicted for short bunches by Equation 2 – see Figure 2.

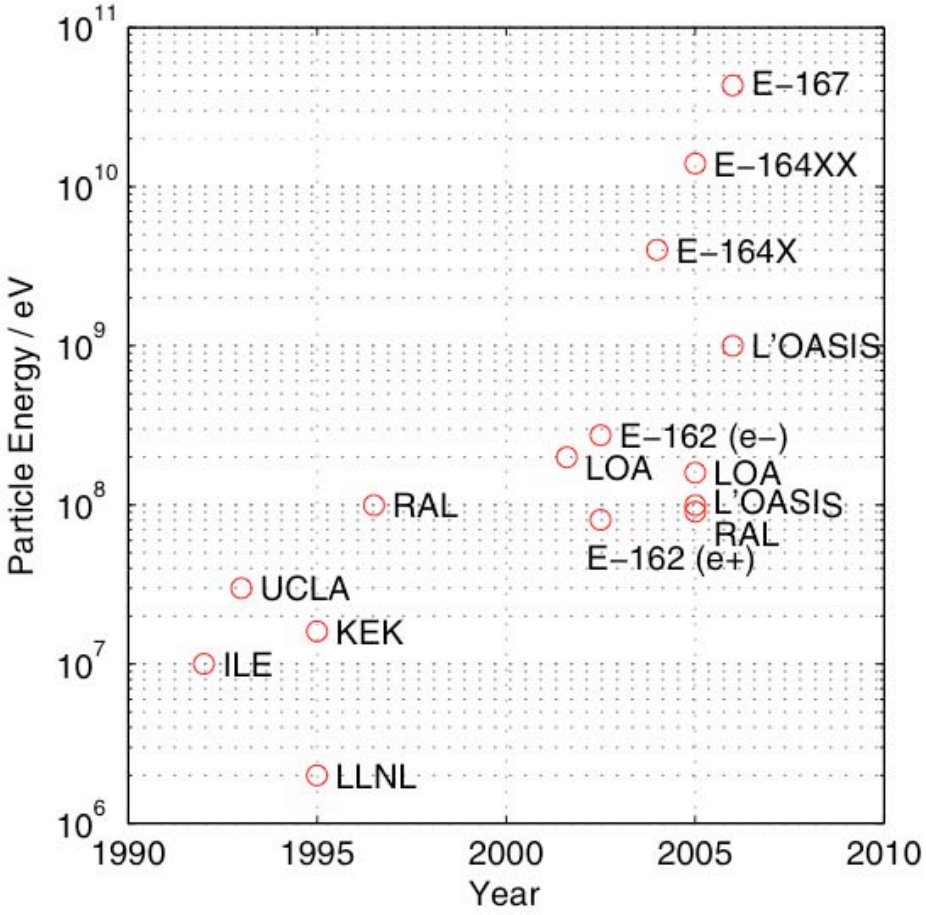

Figure 2: The maximum energy achieved by plasma based accelerator experiments is plotted versus time.

Computer Simulations

As stated before, current and proposed experiments operate in a regime where the linear plasma theory is not valid. To help interpret the experimental data and design new experiments, we have developed extensive computer simulation capabilities that allow us to perform one-to-one modeling of the experiment in this non-linear regime. Two codes are used, OSIRIS [8] and QuickPIC [9]. OSIRIS is a 3-D, fully electromagnetic, relativistic, parallelized particle-in-cell (PIC) code that has been benchmarked against other codes and model problems that can be solved analytically. QuickPIC is a 3-D,

parallel particle-in-cell code that uses a quasi-static approximation to decreases the computing time. OSIRIS and QuickPIC include the effects of field ionization and electron energy loss due to radiation from oscillations in the ion column. OSIRIS and QuickPIC are now the standard tools for simulating the beam plasma interactions in our experiments and have successfully predicted many of the observed phenomena in a quantitative manner.

Plasma Production by Field Ionization

The preceding equations show that producing large amplitude wakefields requires short, high-density electron bunches. If the current density is high enough, the Coulomb field of the relativistic electron bunch can also create the plasma. With a sufficiently dense bunch, the ionization is accomplished by the leading particles of the bunch, such that the majority of the bunch encounters a fully ionized plasma (see Figure 3). Field ionization has several advantages over other techniques, most notably that it allows for the production of long, uniform, high-density plasmas with no timing or alignment issues.

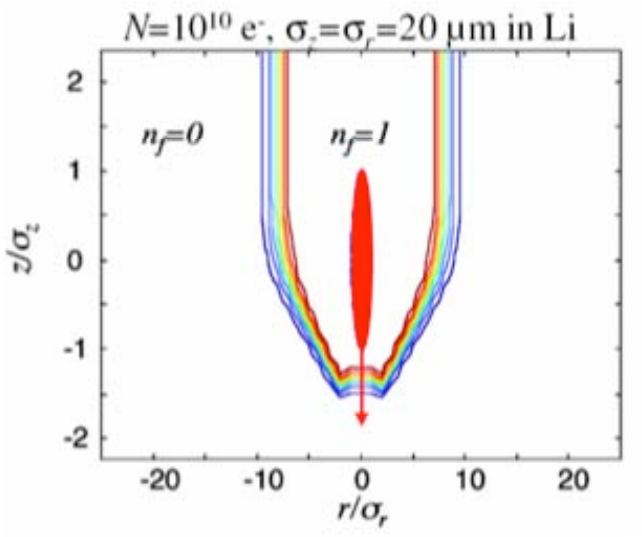

Figure 3: Ionization contours for a Gaussian beam calculated using ADK theory. The electron beam is shown in red. The fractional ionization is noted as n_f. The contour lines indicate that a full ionization is achieved at a position 1.2σ before the center of the bunch, and up to many beam radii.

There are two aspects to achieving the high current densities needed for a field ionized plasma – a high peak current and small transverse size. The high peak current will be achieved in SABER by making use of a threefold compression process similar to what was used for the FFTB experiments (see section 4). A final focus system will deliver beams with a transverse size similar to what was available in the FFTB, ~5μm r.m.s..

A result of these experiments is shown in Figure 4: some of the electrons doubled in energy in just 85cm. SABER will produce beams with properties similar to those that have worked successfully in the past and will allow this work to continued. Table 2 shows the standard operating parameters expected for the E-168 experiment in SABER. Highlights of the experiments E-157, E-162, E-164, E-164X and E-167 are presented in appendix A. In addition to these beautiful physics results, the collaboration has developed a unique apparatus for studying beam-plasma interactions, described in Section 4. The majority of this apparatus will be relocated to the SABER facility allowing these experiments to pick up where they left off.

Table 2: E-168 operating parameters in the SABER.

Mean energy (GeV)	28.5
Energy Spread (full width)	4%
Energy Spread (r.m.s.)	1.5%
Bunch Length (σ_z, μm)	~ 20
Bunch Radius (σ_r, μm)	~ 10
N electrons/bunch	$1.8 \cdot 10^{10}$
Typical Plasma Density (cm^{-3})	$0.5 – 3.5 \cdot 10^{17}$
Typical Plasma Length (cm)	30-120

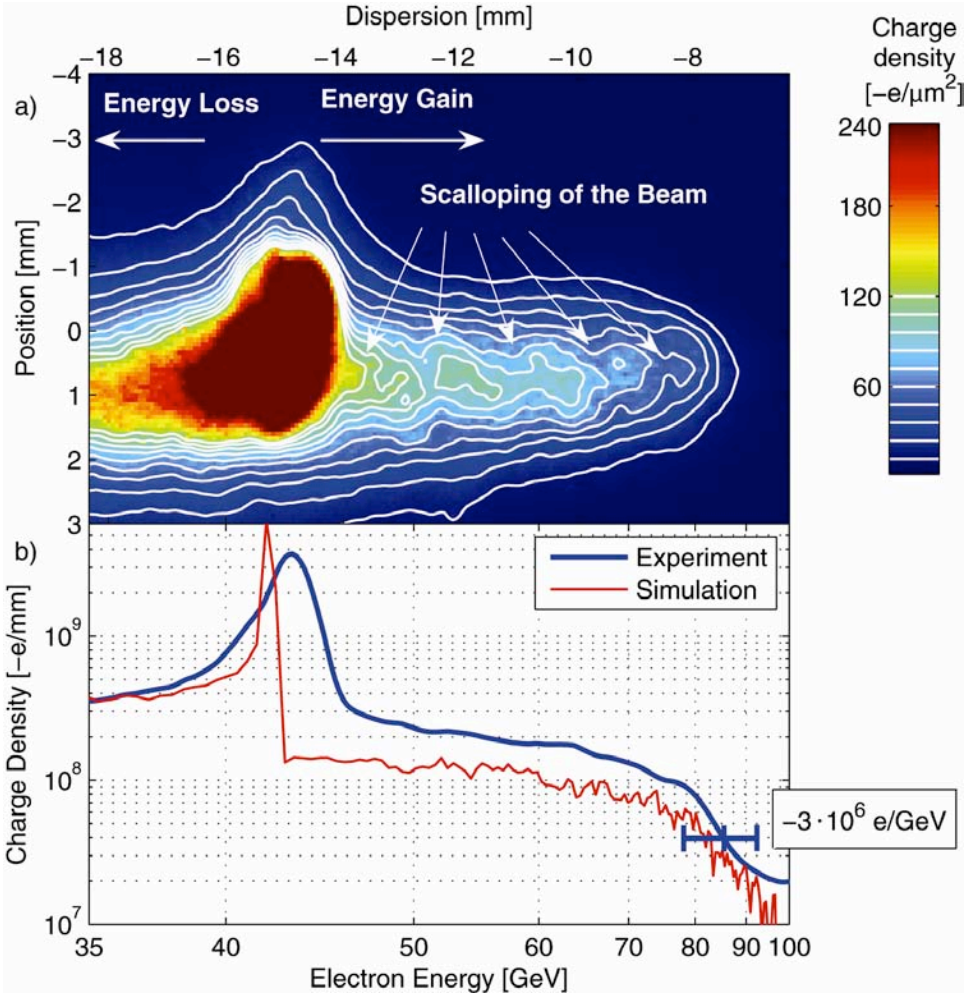

Figure 4: a) Energy spectrum of the electrons in the 30-100 GeV. The image is shown with a colour map that saturates at −240 e/μm^2. The dispersion (shown on the top axis) is inversely proportional to the particle energy (shown on the bottom axis. The head of the pulse, which is unaffected by the plasma, appears at −15 mm, equivalent to 43 GeV. The core of the pulse, which has lost energy driving the plasma wake, is dispersed partly out of the field of view of the camera. Particles in the back of the bunch, which have reached energies up to 85 GeV, are visible to the right. The pulse envelope exits the plasma with an energy-dependent phase advance, which is consistent with the observed scalloping of the dispersed beam.(b) Projection of the image in Figure 2a, shown in blue. The simulated energy spectrum is shown in red. The differences between the measured and the simulated spectrum near 42 GeV are due to an initial correlated energy spread of 1.5 GeV not included in the simulations.

3 Proposed Next Experiments

3.1 Energy Gain

Initial experiments at SABER will use the same long high-density plasma with the lower energy 28.5 GeV electron beam to study the physics beyond energy doubling before head erosion becomes significant. The measurements proposed in E-168 will address several of the key questions emerging from the E-167 energy gain data:

- Can the energy of the particles be more than doubled?
- How does the transformer ratio vary with plasma length?
- What is the maximum percentage of the incoming beam energy that can be extracted into the plasma wake?
- Are there optimum incoming beam conditions (bunch length, spot size) that maximize the transformer ratio and energy extraction?
- Will the electron hose instability eventually become a limiting factor?

3.1.1 Background

The experiments E-157, E-162, E-164, E-164X and E-167 have shown that a plasma can sustain very large electromagnetic fields and that this field can be used to accelerate particles to very high energies in meter long plasmas. Initial efforts at SABER will pick up from where E-167 in the FFTB left off. E-167 used a lithium plasma with a density of 2.7E17 e-/cm^3 to double the energy of some of the incoming 42GeV electrons in just 85cm. simulations indicate that the maximum energy gain was limited by an erosion of the front of the bunch that prevented the bunch from driving a large amplitude wake after about 85cm of plasma, even though there was still significant stored energy in the drive beam (see Figure 5). To understand head-erosion, consider that the front of the beam expands according to its emittance, as it is not subjected to a focusing force, since the plasma and the ion column are not yet formed. This expansion decreases the local beam density that moves the ionization front backward in the beam frame. Eventually the beam electric field drops below the threshold for plasma formation, terminating the wake excitation and the acceleration processes before the energy of the drive beam is depleted.

For the parameters of our experiments, the plasma wavelength and the bunch size in all three dimensions are on the same order. For this regime, there exists no analytic description of the dynamics of the plasma wakefield; therefore, it has to be addressed through experiments and computer simulations. Simulations are used to understand the maximum electron energy observed in the experiment. Figure 4b shows a comparison of the measured energy spectrum with one derived from simulations. The electron current distribution is extracted from the energy spectrum of the beam measured upstream of the plasma and by comparing it to a phase space simulation using the code LiTrack [10]. The wakefield from this current distribution and the propagation of the bunch through the plasma are modelled using the 3-dimensional, parallel particle-in-cell code QuickPIC. QuickPIC includes the effects of field ionization and electron energy loss due to radiation from betatron oscillations of the bunch electrons in the ion column.

Figure 5a and Figure 5b show the simulation output at two different positions along the plasma. At a distance of 12 cm, the wake produced by the motion of the plasma electrons resembles that produced in a preformed plasma, since the ionisation occurs near the very head of the beam. All the plasma electrons witness the space charge field of the ion column and are pulled back toward the beam axis. This results in a radial current that not only sets up an electron density spike behind the bunch, but also creates a longitudinal electric field that accelerates the particles at the back of the electron bunch. After 82 cm one can see the effect of beam head erosion in that the ionization front now occurs further back along the bunch. Even though the wake is formed further back, the peak-accelerating field occurs at approximately the same position along the bunch. However, the modified ionization front causes some blurring of the position where the returning plasma electrons arrive on the axis, an effect known as phase mixing. This not only reduces the peak accelerating field but also leads to some defocusing of the high-energy beam electrons in this region. The simulated energy distribution at this point has been binned equivalently to the experimental data, as shown in Figure 4b. The quantitative agreement between the two spectra is good. In the simulations, electrons are accelerated to a maximum energy of 95 GeV. In the experiment, the maximum detectable energy is determined by the spot size at the detection plane (for a given detection threshold), and the highest detected energy is 85 GeV. For the present case,

this corresponds to a detection threshold of $3 \cdot 10^6$ electrons per GeV. The electron energy of the bin containing $3 \cdot 10^6$ electrons/GeV in the simulations is shown as a function of position along the plasma is Figure 5c. Also shown are maximum energies measured in the experiment at 85 and 113 cm for similar electron current profiles.

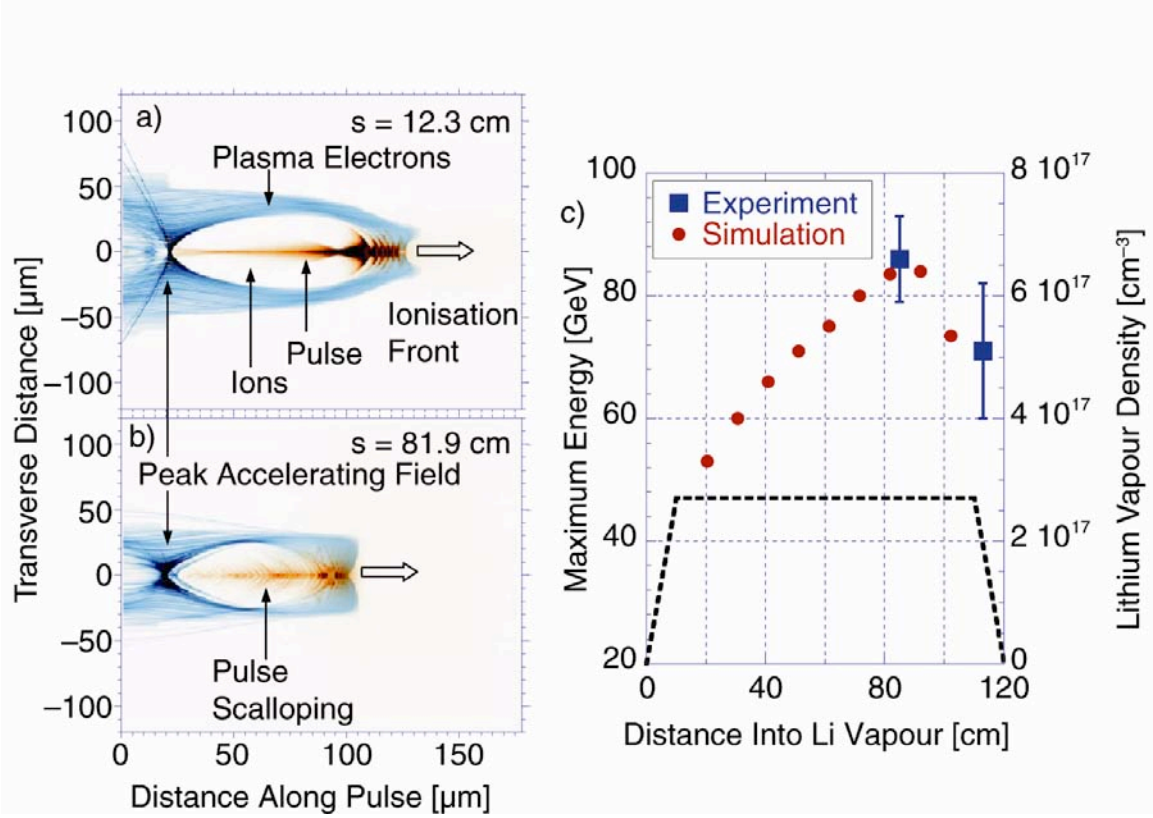

Figure 5: **Simulation of the electron bunch (red) and the plasma electrons (blue) at approximately 12 cm (a) and 82 cm (b) into the plasma. The bunch travels from left to right. The scalloping features seen at the front of the bunch in (a) are the result of an increasing focusing force as the plasma electrons are still being blown out by the beam electrons. The back of the bunch however is nearly uniformly focussed by the plasma ions. The scalloping of the bunch in (b) is due to the energy-dependent focusing through the ion column.(c) The maximum observed energies in E-167 (blue squares) for two different plasma lengths is compared to the energy of the particle bin containing $3 \cdot 10^6$ electrons/GeV in simulations (red dots) as a function of distance in the laboratory frame. Also shown is the lithium density used for the simulations (dashed line).**

The energy in the simulations increases approximately linearly with propagation distance up to a value of 80 GeV at about 70 cm and then saturates at 85 GeV at 85 cm due to the phase mixing effect which leads to gradual defocusing of the highest energy electrons as mentioned above. As the beam propagates beyond 85 cm, the highest energy electrons continue to be defocused so much so that at 104 cm a significant number of the high-energy electrons are lost to the simulation walls causing the maximum observed electron energy to drop to 60 GeV. In the experiment electrons defocused at the angles seen in the simulations would not be captured by the electron spectrometer. It should be noted that no significant wakefield is left beyond 104 cm, as the electron beam core containing the bulk of the particles is completely eroded away.

3.1.2 Proposed Measurements

Head Erosion

Experiment E-167 demonstrated that the front of a high energy, high peak-current electron beam can produce ≈50GeV/m wakefields in a plasma, sustain them for a distance of roughly one meter, and use them to accelerate particles in the back of the same bunch. More specifically, a plasma was used to double the energy of some of the initially 42GeV electrons in just 85cm. A longer plasma of 113cm was also studied, but surprisingly yielded a lower maximum energy. Computer simulations have identified head erosion as the likely mechanism limiting the energy gain and this interpretation agrees with the experimental results presented in the previous section. Simulations suggest that using either a lower emittance drive beam or a pre-ionized plasma can reduce or eliminate head erosion as an obstacle limiting the energy gain and extracting more energy from the bunch. Simulations using the beam parameters expected to be available at SABER indicate that we can produce accelerating gradients similar to those in E-167 and use the 28.5GeV beam to probe the physics issues encountered in the regime beyond energy doubling (see Figure 6).

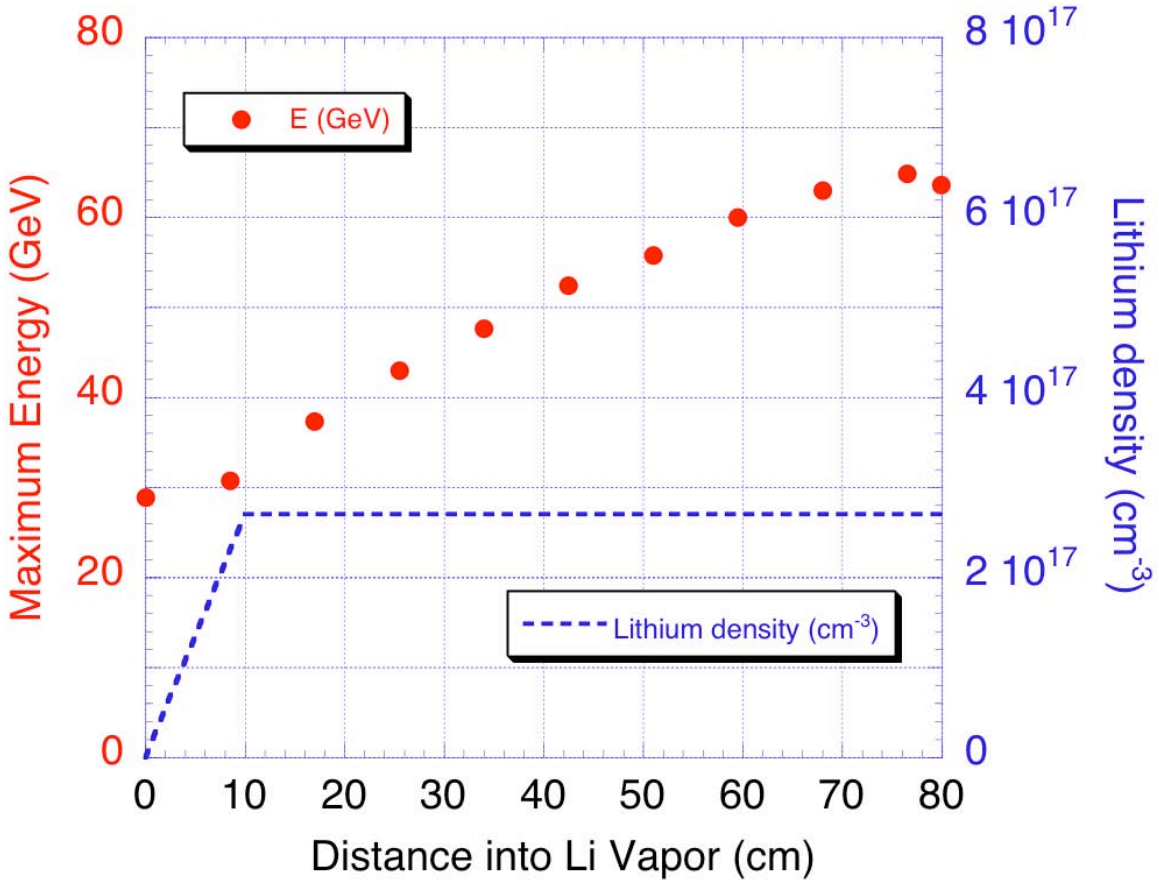

Figure 6: An output of QuickPIC simulation with nominal SABER parameters. The maximum energy gain occurs about 70cm into the pure lithium column. The optimum values for the waist size and location of the incoming bunch are currently being studied.

Transformer Ratio & Efficiency

For the same bunch where particles reached a maximum energy of 85GeV, particles reached a minimum energy of only 13GeV. For a Gaussian bunch the ratio of the maximum accelerating field to the maximum de-accelerating field can be at most two [11]. The measured value of 43/29 = 1.5 is substantially lower. For the 113cm plasma the value was even lower. In addition, the nature of the wake evolution in computer simulations (see next section), indicates these values are perhaps an overestimate. For experiments E-157/E-162/E-164/E-164X the energy change from the plasma was on the order of the incoming energy spread, and it was not possible to quantify the transformer ratio. The initial E-167 runs resulted in much larger energy gains, but the imaging magnetic spectrometer used to measure the energy spectrum did not transport the low

energy electrons and again it was not possible to quantify the transformer ratio. The final E-167 run implemented an alternate technique to measure the entire energy spectrum (see section 4, Figure 17) and successfully measured energy doubling in the finite time remaining in the FFTB. E-168 will complete the data and systematically measure the transformer ratio as a function of plasma length, incoming bunch length and beam radius to optimize the transformer ratio and thus the efficiency.

While the minimum energy particles measured were only 13GeV, the mean energy of the bunch was still ~30GeV indicating that more than half of the initial beam energy remains to be exploited. Using a lower emittance beam or pre-ionizing the plasma are not immediately practical for the initial runs in SABER. E-168 will use the lower energy (28.5GeV), high peak current SABER beam to maximize the percentage of extracted energy before head erosion becomes a limiting factor. See Figure 6 with latest from Miaomiao.

Electron Hose Instability

It has been suggested that instabilities such as the electron hose instability may become a limiting factor in the application of plasma wakefield accelerators in high energy colliders [12]. Such applications will require long, high-density plasmas where the total number of betatron periods will be in excess of 100. There has been no experimental evidence to date that such instabilities are limiting performance. By maximizing the plasma density-length product we can maximize the number of betatron periods experienced by the drive beam and continue to expand the boundaries where the PWFA process works stably.

3.2 Trapped Electrons

A striking new phenomena emerged when our experiments began producing wakefields greater than ~10GeV/m – trapped electrons. This trapped charge can have potentially adverse effects on the accelerated particles. In addition to their impact on the primary electron beam however, there is evidence that the trapped electrons may themselves have interesting properties such as multi-GeV energies, better emittance than the primary beam and bunch lengths of 10's of femtoseconds. A major component of the E-168 program will be to further our understanding of trapped electrons. Specifically:

- What is the mechanism?
- Do the properties of the trapped electrons depend on the ionization potential of the buffer gas?
- What are the properties of the trapped charge: energy, emittance and bunch length?
- Can the particle trapping be suppressed?
- Do the trapped electrons load the accelerating portion of the wake reducing the maximum energy gain?

3.2.1 Background

During the acceleration experiment a number of measurements indicated that the total charge that exits the plasma is larger than the incoming bunch charge when the electron bunch length is made shorter and shorter (and at the same time the peak current larger and larger) and the wake amplitude is made larger and larger. These measurements include an excess of charge as measured by a toroid located about 70 cm downstream from the plasma, the emission of light with a continuous spectrum on top of the spectral lines of the neutral lithium (Li I), and a large excess of light on the profile monitor downstream of the plasma. In these measurements the amount of charge and light are also larger with shorter, higher current bunches.

We have demonstrated experimentally that electrons can be trapped and accelerated by the plasma wake when the wake amplitude exceeds a certain threshold. Simulations indicate that the trapped particles are plasma electrons born inside the wake itself through field ionization of the helium (He) mixed with the lithium (Li) in the He to Li transition region of the heat-pipe oven. Ionization of the He electrons occurs when the Li plasma focuses the bunch and its radial space charge field exceeds ≈70 GV/m. Calculations show, and simulations confirm that the Li electrons born in the front of the bunch have a much larger trapping threshold (13). The trapped particles are quickly accelerated to relativistic energies, are focused by the plasma ion column, and form a short bunch near the peak of the accelerating field. On one hand, these trapped particles may have very interesting properties, as discussed earlier in this proposal: small spatial

dimensions with features < 1 μm, low emittance, and high peak current and brightness that could make them interesting for light source applications.

On the other hand, trapping of plasma electrons is equivalent to the dark current of RF accelerators and can create unwanted, low energy particles in the accelerator. Depending on the number of trapped electrons and on the energy they acquire, these electrons could load the plasma wake and therefore degrade the quality of the accelerated beam, or even reduce its energy gain. In preliminary simulations this beam loading can result in a energy gain lower by 40% than compared to the same simulation without He, and therefore without trapped particles. Current energy gain results do not show clear evidence of strong wake loading, however, in the experiment it is not possible to remove the He buffer gas from the oven. It is therefore not possible at this point to determine the effect of trapped particles beam loading on particle acceleration. However, trapped particles can reach energies comparable to the drive bunch energy over an energy-doubling plasma length, and self-injected (not strictly trapped) particles have a broad energy spectrum.

Whether we are looking to exploit some of the potentially interesting characteristics of trapped electrons or eliminate them all together, it is important to understand their origin and characteristics.

3.2.2 Proposed Measurements

Dependence on Ionization Potential of Buffer Gas

Simulation codes that include the ionization and that can model the full-scale experiment in a reasonable amount of time have recently been developed by our collaboration. Simulations indicate that helium electrons are trapped in the transition region between the helium buffer gas and the lithium vapor. A way to test this is to exchange the helium buffer gas with another noble gas; neon, for example. Since neon has a different ionization potential, it will be field ionized at a different position in the wake than the helium. The neon electrons would then be trapped at different positions in the wake than the helium electrons or may not even be trapped. For equivalent incoming beam parameters, the energy and quantity of trapped electrons will be measured for

several species of buffer gas. Any correlation in energy or amount of trapped electrons with the change of buffer gas would support that the trapping occurs from the buffer gas.

Beam Loading & Backgrounds

In the present experiment a large amount of charge is lost along the beam line. In a future plasma afterburner these particles would extract energy from the plasma wake, thereby reducing the afterburner efficiency. They could also be the source of additional particles and radiation background. A means to suppress this particle trapping must be devised.

We propose to demonstrate that this trapping can be avoided by keeping the peak bunch radial field below ~5 GV/m (the field ionization threshold on the time scale of the $\sigma_z \approx 20$ μm drive bunch for the first Li electron) in the He to Li region of the oven. The peak bunch radial electric field is a function of the location of the beam waist – see Figure 7. To eliminate trapping at the plasma entrance He-Li boundary, the beam waist will be placed sufficiently far into the Li zone to avoid ionization. For the current 1.2 meter-long plasma source, we can adjust the beam waist to not ionize for as much as the first 60cm of the pure Li column and still double the energy of some electrons. If successful this experiment would not only show that trapping can be avoided, but would also demonstrate the fact that the trapped particles indeed originate from ionization of He, a fact so far only inferred from simulations. Additionally, the measured energy gain and accelerating gradient could increase by 10 to 40%, depending on the actual wake loading. This could bring the average accelerating gradient in the 50 to 60 GV/m.

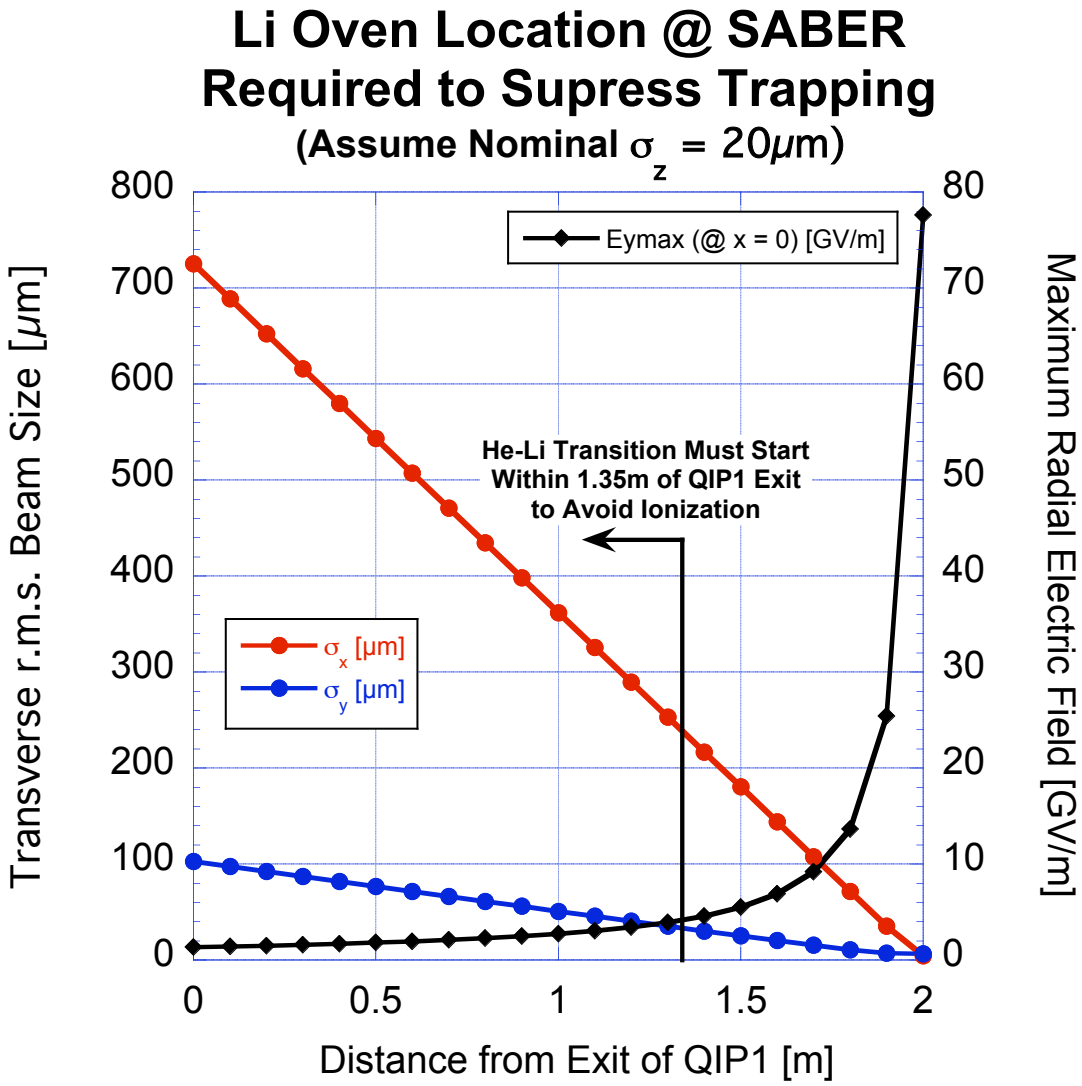

Figure 7: A plot of the beam size and peak radial electric field from the exit of the final focusing quadrupole to the nominal plasma entrance. By placing the plasma waist sufficiently far into the pure lithium column we can eliminate the trapped particles originating at the entrance helium –> lithium boundary.

3.3 New and Improved Diagnostics

The experimental results summarized in Appendix A were made possible by the continual development of specialized diagnostic tools: Optical Transition Radiation (OTR) profile monitors, time-integrated and time-resolved Cherenkov light profile monitors, non-invasive energy spectrometers, and broad-band terahertz power meters to

monitor CTR radiation to name a few. These have been developed to quantify the inner structure of the bunch, which depends critically on the stability of various accelerator components. For example, the bunch length is influenced dramatically by modest phase changes in the accelerating cavities: if the bunch has its shortest possible length in SABER (~20 μm r.m.s.), an RF phase error of 0.5-degrees S-band in the sectors 2-6 of the linac induces a relative bunch length change of more than 50%, with the chicane energy feedback switched on.

The experiments listed in the previous sections will benefit from additional diagnostic capabilities. Data with the plasma source inserted in the beamline is acquired at a rate of 1Hz. Tuning up the linac to give the optimally compressed pulses with good transverse emittance is more readily accomplished at 10Hz. Many of our diagnostic CCD cameras are cooled for a high dynamic range to help us monitor subtle details of the beam profile or spectrum. Although very sensitive, these cameras have mechanical shutters that prevent them from working reliably at 10Hz. We are in the process of upgrading several of our cameras to models with electronic (not mechanical) shutters that can monitor the beam at 10Hz and aid in tuning up the beam. By placing three distinct cameras at appropriate locations, we will be able to measure and minimize the incoming transverse emittance. Monitoring the incoming emittance on a pulse-to-pulse basis will be critical for interpreting the data emerging from the plasma in regimes where the head erosion is a significant factor.

Equation 2 indicates the amplitude of the accelerating wakefield scales like the inverse of the bunch length squared. To first direct measurement of the ultra-short bunches was through a THz autocorrelator that was initially constructed during the E-164X runs but has been continually improved. At maximum compression, the electron bunch profile is nearly Gaussian and symmetric. Much of the plasma data is taken with the beam deliberately not at maximum compression when the beam is predicted to have an asymmetric shape consisting of a relatively long low-current ‘trunk’ or ‘tail’ and a high-current relatively symmetric central core. The autocorrelation of the beam pulse is an inherently symmetric function and thus will not provide detailed information about asymmetries in the longitudinal pulse shape. However, it is a relatively simple diagnostic, which provides an average measurement of the high-current core of the

bunch. The existing autocorrelator is shown schematically in Figure 14. The autocorrelation traces shown in Figure 15 indicate the maximally compressed bunches in the FFTB were in the 10-20 μm r.m.s. range predicted by simulations. The dynamic range of this device is currently limited by the THz properties of the materials used for beam windows and splitters. We will investigate the dynamic range of this device with alternate material beam windows and beam splitters to improve on the dynamic range measured thus far. Finally, we are in the design stages of a more advanced single shot autocorrelator that will use a modified design in conjunction with a segmented detector to make this measurement for each individual bunch.

4 Existing experimental apparatus

The plasma wakefield acceleration experiments will be conducted in the SABER beamline in the beginning of the SLAC Linear Collider (SLC) South Arc. The plasma will be located at the focal point of the SABER beamline. The complete setup is distributed along roughly 75m of the beamline. Figure 8 shows the schematic of the experimental set-up after our apparatus has been relocated from the FFTB.

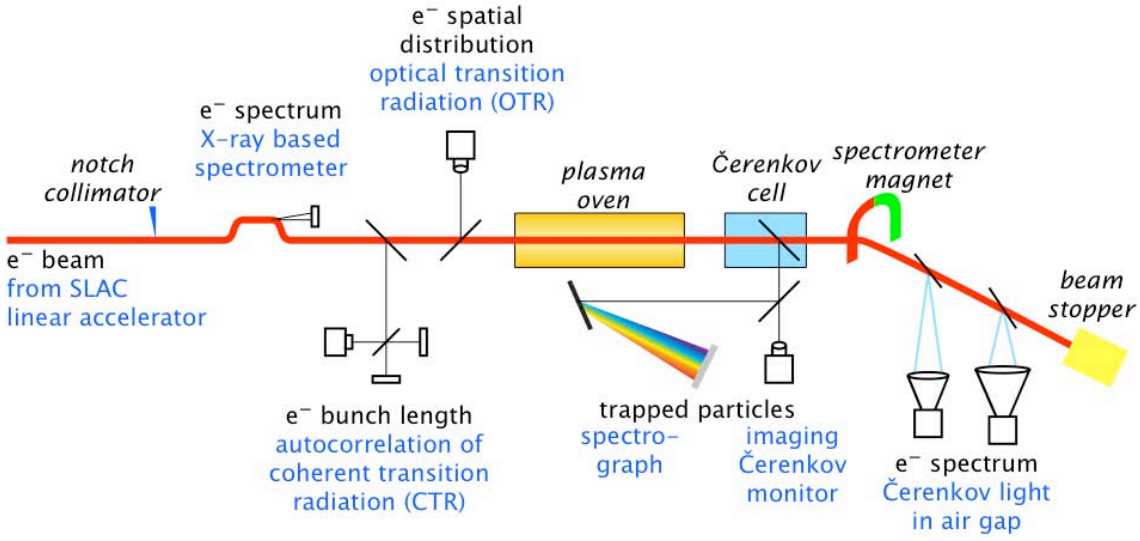

Figure 8: Schematic of the experimental layout.

4.1 Beamline

In the summer of 2002, SLAC installed a new bunch compressor chicane for the SLAC linac at the 9 GeV beam energy point (1/3 way down the linac). Prior to installation of the chicane, the electron bunches had a typical length of 650 μm r.m.s.. With the chicane, the bunch is compressed in stages to a predicted minimum of ~18 μm. The compression process proceeds as follows. The initially 6 mm long 1.19 GeV bunch in the North Damping Ring is compressed to 1.3 mm in the transition from the damping ring to the linac (RTL). Once in the linac the bunch is given a correlated energy chirp as it is accelerated up to 9 GeV where it is compressed using the magnetic chicane to ~140 μm. In the remaining 2 km of linac the bunch is further accelerated to 28.5 GeV; here, wakefield effects introduce a further chirp which is used in the south arc to compress the bunches to a length as short as 18 μm (45 fs) rms.

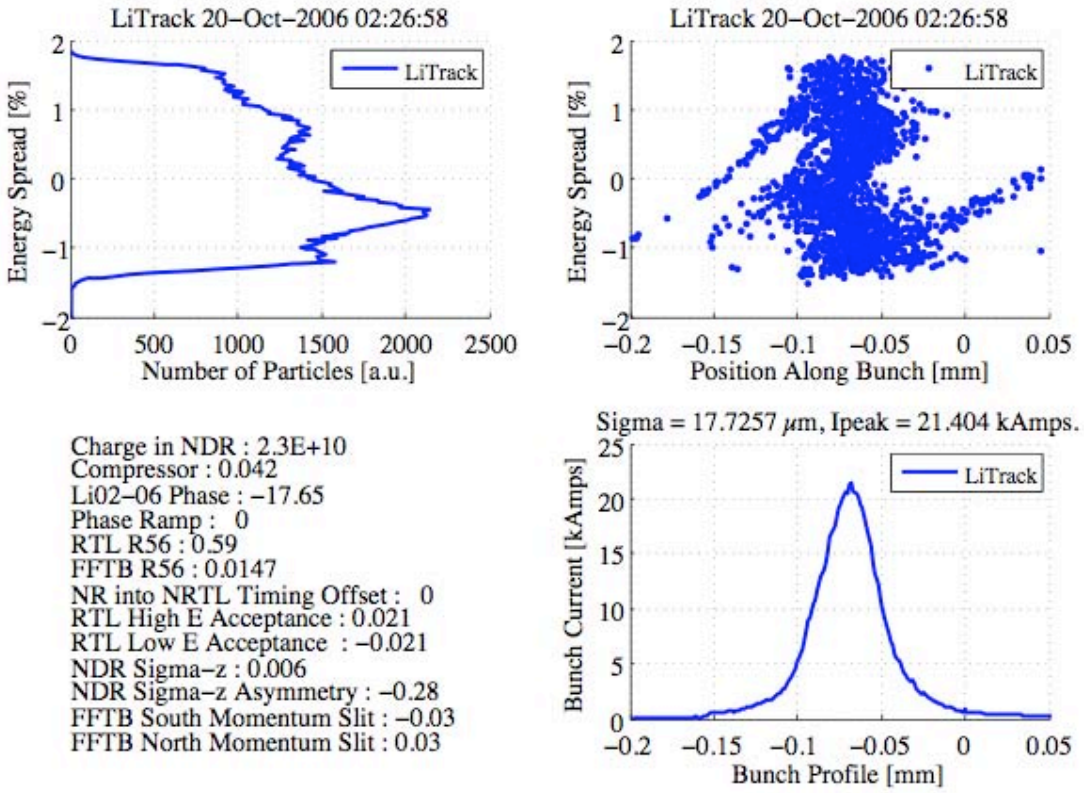

Figure 9: Expected longitudinal phase space at SABER IP-0, simulated using the code LiTrack.

In the beam switchyard just before the start of the south arc, a weak magnetic chicane located in an energy dispersive plane produces a synchrotron radiation stripe with a profile equal to the bunch energy spectrum. The radiation stripe is intercepted by an off-axis phosphor screen yielding a pulse-to-pulse non-destructive measurement of the incoming energy spectrum. This device is described in more detail in Section 4. The plasma will be located in the SABER focal point region. Here, the 28.5 GeV electron beam is focused to a size of the order of 5 μm r.m.s. – see Figure 10. The aspect ratio and location of the beam waist are adjusted with the final doublet (quadrupole pair) before the interaction point.

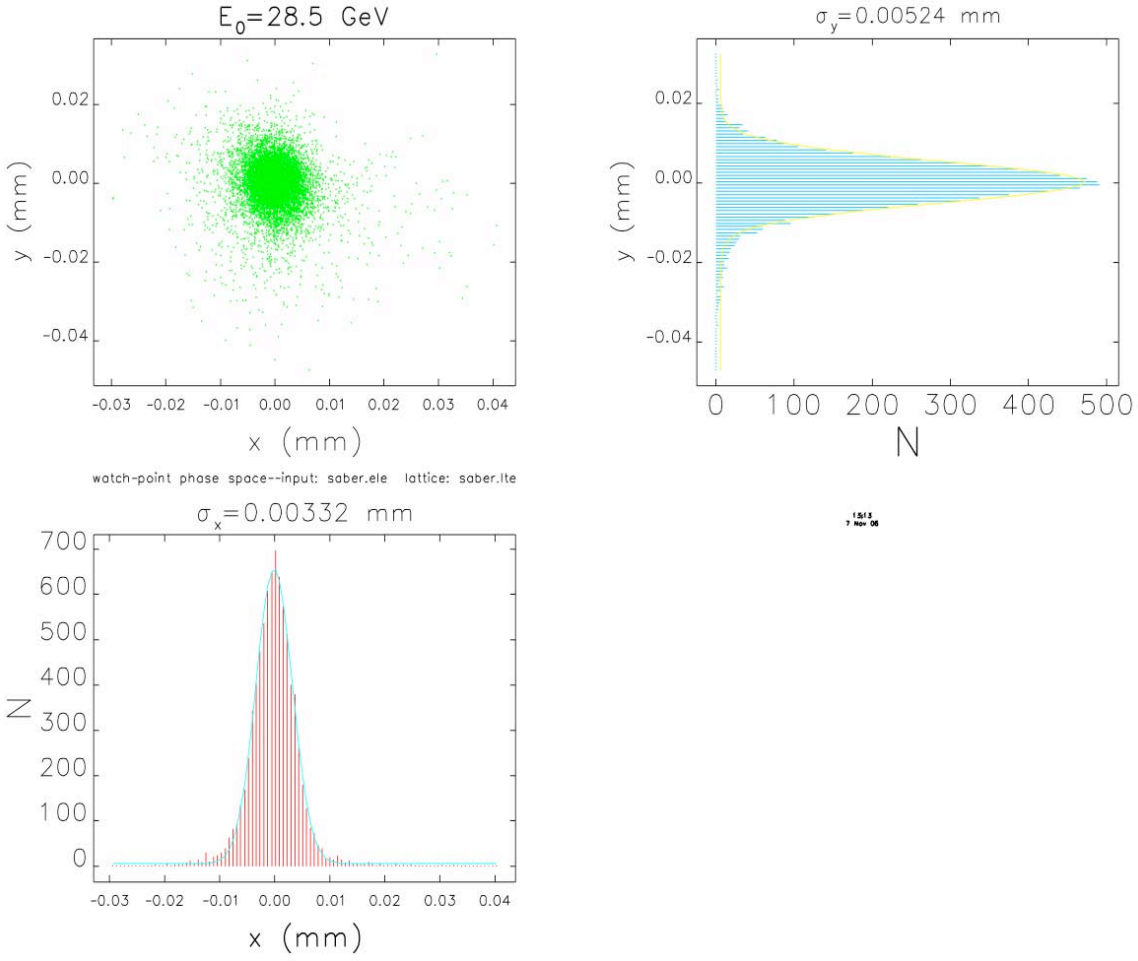

Figure 10: Transverse beam size and projections fitted to a Gaussian for the SABER focal point. The expected spot size (3μm x 5μm) is comparable to the values used successfully in the FFTB.

4.2 Plasma source

We have been using an ionized column of lithium vapor as a plasma source with great success for all the previous experiments. Lithium is used for its low first ionization potential, its low cross-section for collisional ionization and its relatively high second ionization potential. In E-167, the ultra-short electron bunches required plasma densities of $> 2\cdot10^{17}$ e^-/cm^{-3} over 1 meter in length. Such high-density plasmas with required axial uniformity cannot be produced with laser or discharge ionization. We have used the self-fields of the compressed and tightly focused bunch to tunnel-ionize lithium. As the electron bunch is made shorter to increase the accelerating gradient of the PWFA module, its radial space charge field also increases. For a bunch with a Gaussian profile in r and z, the maximum electric field, measured in GV/m, is given by:

$$E_{r,\max} \approx 5.2\cdot10^{19} N/\sigma_r\sigma_z \qquad (3)$$

where N is the number of particles in the bunch, and σ_r and σ_z are the r.m.s. bunch sizes in the radial and axial directions, measured in meters. This maximum field is reached in the middle of the bunch (z=0), and at $r \approx 1.6\ \sigma_r$. This field can exceed the threshold for field-, or tunnel-ionization of the vapor in which the bunch propagates. The threshold for field-ionization depends on the ionization potential of the atoms φ, and on the bunch length and is of the order of 6.8 GV/m for lithium (φ = 5.4 eV) and a bunch length of ≈20μm. With short bunches the threshold can be exceeded over a large enough volume that the self-ionized plasma is similar to a pre-ionized plasma for the wake excitation.

The fractional ionization created by a σ_r = 15 μm, σ_z = 20 μm bunch with $N = 10^{10}$ electrons is shown in Figure 3. The ionization process is essentially a threshold process, and therefore full ionization of the vapor's first valence electron is reached up to $\approx 2\sigma_z$ ahead of the bunch, and up to ≈110 μm radially. For such a short bunch the optimum plasma density for wake excitation, as given by the linear theory, is $\approx1.3\cdot10^{17}$ cm^{-3} , and the plasma electrons are expelled to a radius smaller than the plasma radius of 110 μm. A wake amplitude similar to that driven in an infinite pre-ionized plasma can thus be expected in this case. Since the transverse focusing force of the plasma wake allows for the channeling of the electron bunch over many beam beta functions, meters-long, self-ionized PWFA modules may allow for large energy gain in single high-gradient PWFA

modules. The self-ionization process could suppress the need for staging of PWFA modules to achieve large energy gains.

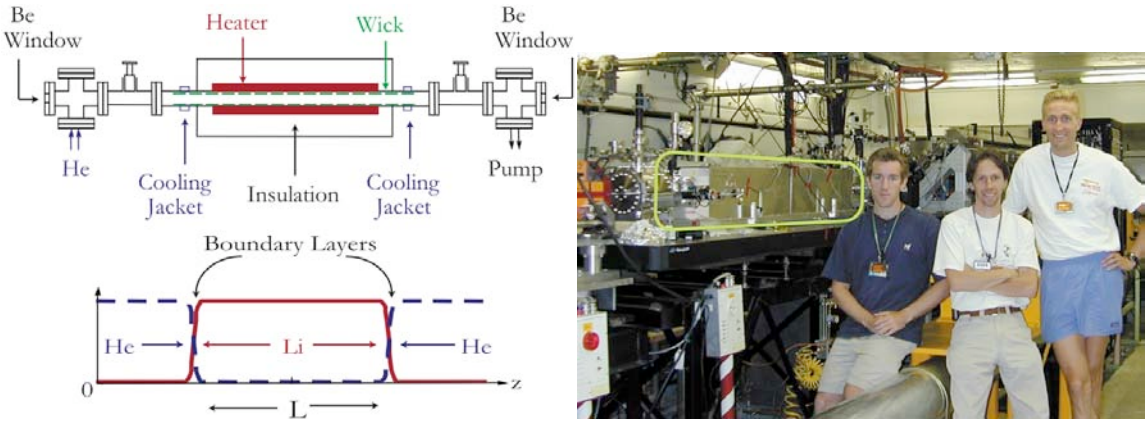

Figure 11: The plasma oven, in a schematic view (left) and a photograph of the installed oven (right). A buffer region filled with helium is used to confine the plasma.

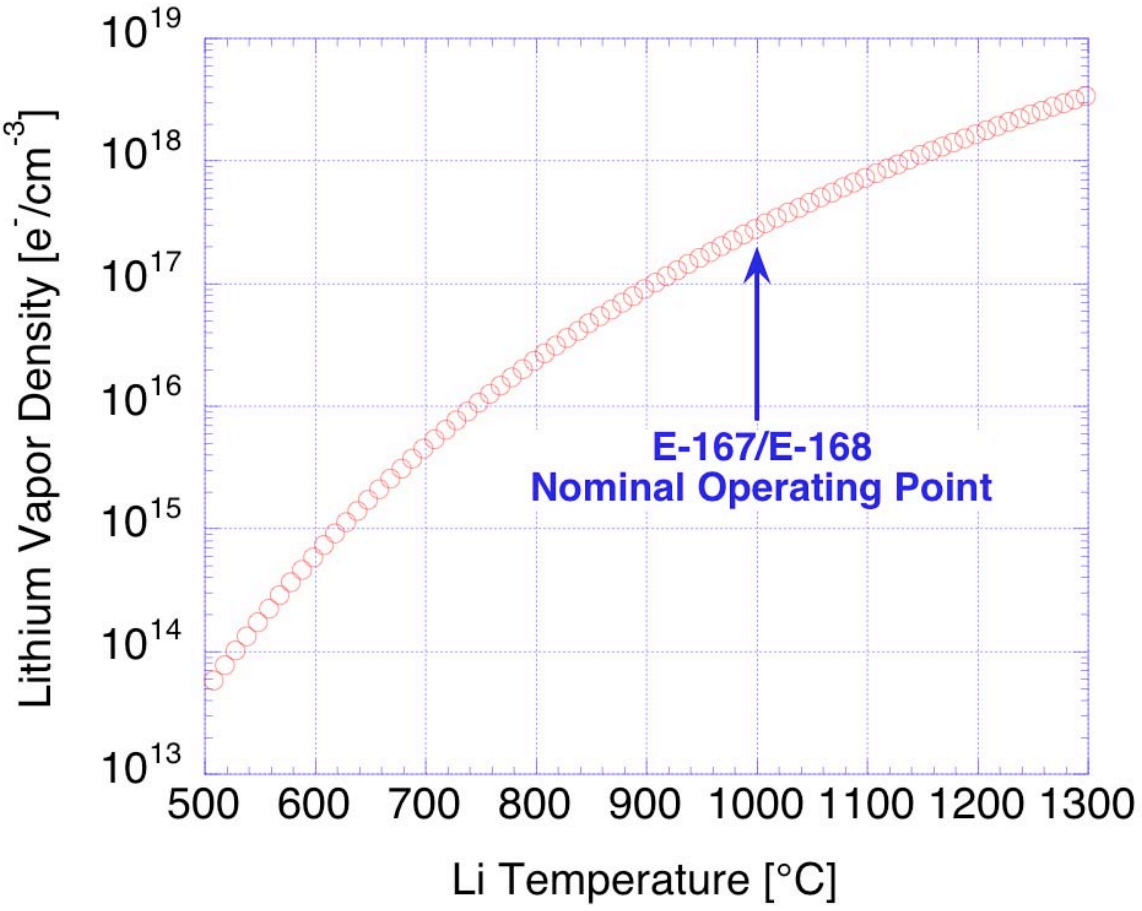

Figure 12: Vapor pressure curve of lithium. The ~$3 \cdot 10^{17}$ e^-/cm^{-3} plasma densities optimum for E-167 & E-168 require the lithium oven to operate at 1,000 °C.

In the self-ionized regime, the plasma density is adjusted through the vapor density, which is very stable in a heat-pipe oven, and is insensitive to shot-to-shot changes of the beam parameters. Figure 12 shows the vapor pressure curve of lithium. A change of temperature from 500° C to 1050° C can lead to a change in vapor density from ~$5 \cdot 10^{14}$ e^-/cm^{-3} to $5 \cdot 10^{17}$ e^-/cm^{-3}. Although it is relatively easy to ionize the first electron of lithium, the second electron has a much larger ionization potential of 75.6 eV that helps to prevent contribution to the plasma density from the ionization of the second electron. The helium buffer gas has an even larger ionization threshold of 293 GV/m. From time to time, it is desirable to have a plasma-off condition. In the past, this was accomplished by turning off the ionization laser. In the beam-ionized regime, this would only be possible by drastically changing the electron bunch parameters. Since this is not desirable, we constructed a pneumatic shuttle system that exchanges the Li oven for a bypass line (a beam pipe filled with the helium buffer gas of the Li oven) in a matter of seconds.

Near the focal point, the SABER beamline is sloped downward at an angle of roughly 4 degrees in the direction of beam propagation. When the lithium oven is hot the strong wicking action within the oven is expected to overcome this slope, however there will likely be some modifications to the oven turn on and cool off procedures as a result. These issues are being investigated with the E-167 heat pipe oven now at UCLA.

4.3 Diagnostics

In addition to the usual SLC beam position monitors (BPMs) and beam current monitors (toroids), we have developed an extensive set of specialized diagnostics. All diagnostics are acquired at 1 Hz and correlated on a pulse-to-pulse basis. For the compressed bunches, the longitudinal bunch profile is strongly correlated to the energy spectrum. A non-destructive spectrometer following an idea developed for the SLC [14] is used to determine the energy spectrum of the incoming bunches (Figure 13). In a horizontally dispersive section in the beam switchyard at the entrance of the south arc, a weak magnetic chicane deflects the beam in the vertical direction and produces a stripe of beam synchrotron radiation. The horizontal profile of this radiation is the energy spectrum of the incoming bunch. To record the spectrum, the radiation is intercepted by

an off-axis phosphor screen. The light from the phosphor is transported and imaged on to a cooled CCD camera with 12-bits of dynamic range located outside of the linac housing. The typical r.m.s. energy spread on the beam is 1.5% or ~ 420 MeV whereas the energy resolution of the x-rays on the phosphor is only on the order of 60MeV. Thus the relative longitudinal current distribution of the electron bunch can be measured from shot-to-shot. These energy spectra are also used to infer the bunch current profile (see here after).

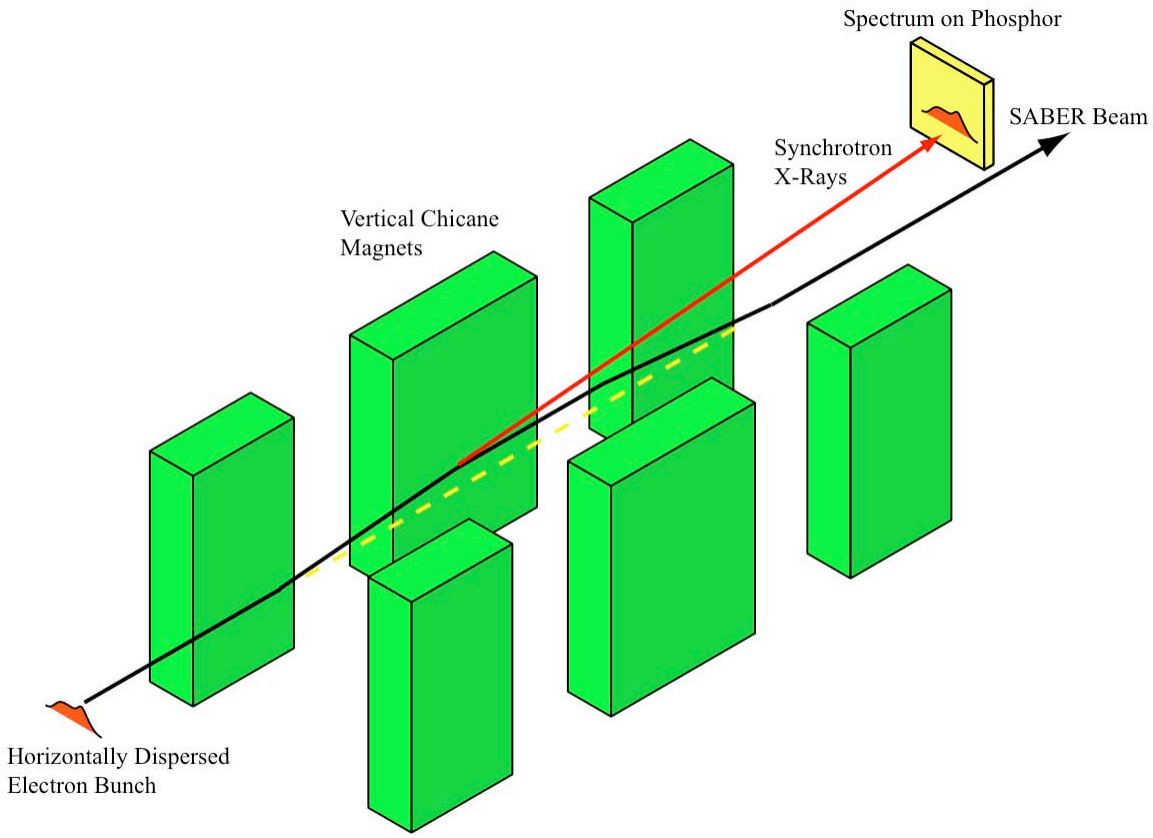

Figure 13: A magnetic chicane, placed in a horizontally dispersive section, is used for a non- invasive measurement of the energy spectrum of the bunch.

Bunch length and profile measurements using transition radiation

When an electron bunch passes though a conducting foil, it emits transition radiation. At wavelengths longer than the bunch length, this radiation is coherent. The

spectrum of this radiation as well as its total power can yield information on the bunch. First, the total energy of the coherent transition radiation (CTR) is inversely proportional to the electron bunch length. As the coherent radiation is in the THz wavelengths for our expected bunch lengths, the energy is measured using a pyro-electric detector. By recording the total CTR energy, the relative bunch length, or peak current, can be monitored on a bunch-to-bunch basis. This allows the shortest bunches to be reached by the experiment. Second, the coherent power spectrum can be indirectly measured using a Michelson interferometer. This setup produces an autocorrelation trace of the CTR signal, which yields an average measurement of the electron bunch profile. Much improvement has been made on this diagnostic over the past experimental runs, and it will be an important part of the effort to ensure we have the short bunches necessary for high gradient acceleration. It will be located upstream of the plasma.

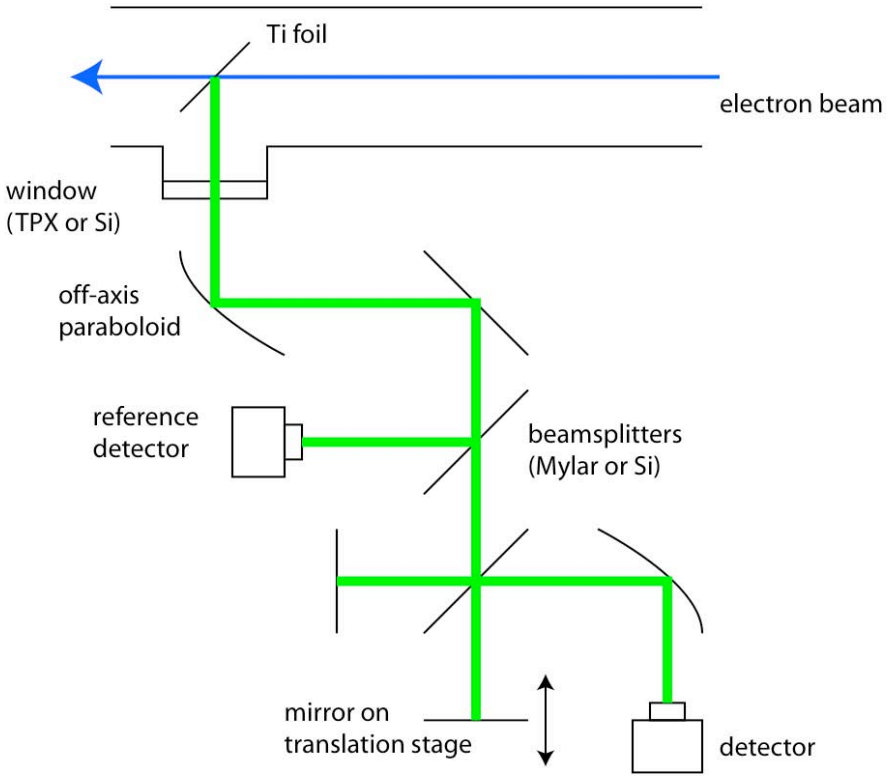

Figure 14: Schematic of the Michelson Autocorrelator setup. The original version used a plastic (TPX) vacuum window and a Mylar (PET) beam splitter. The current version has superior frequency uniformity resulting from using silicon (Si) as both the vacuum window and beam splitter.

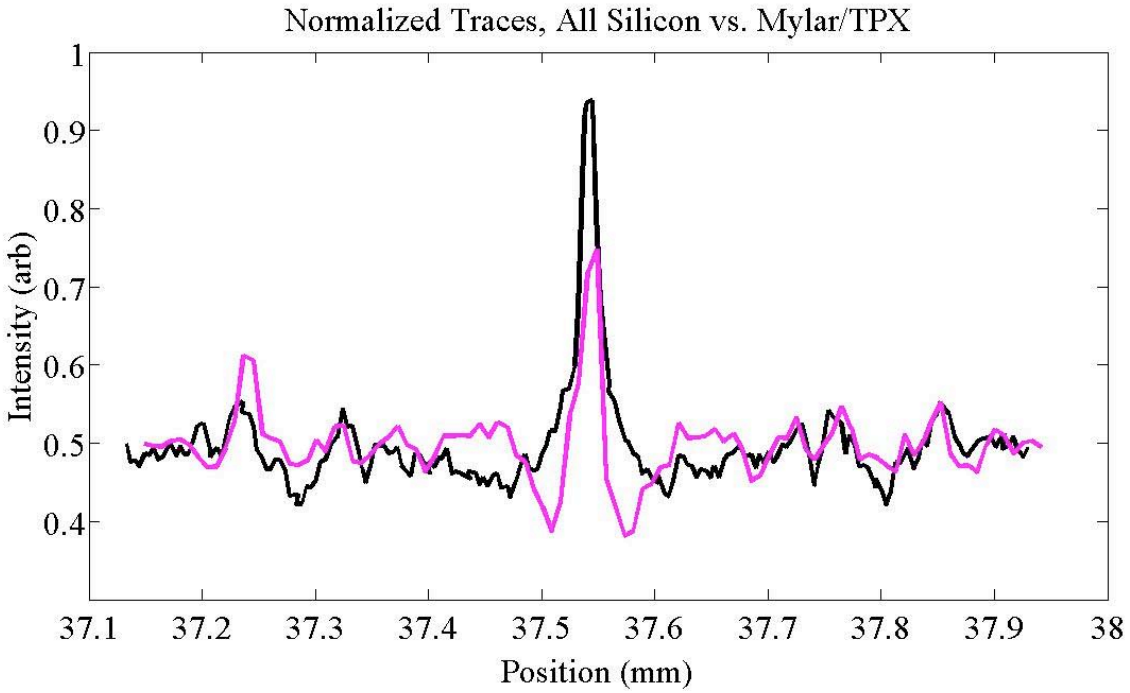

Figure 15: Measured autocorrelation trace of the coherent transition radiation (CTR) that the electron bunch emits when it goes through a titanium foil. The interference is measured with the Michelson interferometer shown in **Figure 14**. Improvements in the materials used led to the reduction of .the influence of the vacuum window and beam splitter material evidenced by the dips on either side of the interference peak on the purple trace. The black curve obtained with a silicon window and beam splitter shows more details of the bunch profile, such as the shoulders on either side of the peak reflecting the presence of a bunch "nose" or "tail".

In addition to the longitudinal profile, the bunch transverse size and position is measured using the optical, incoherent portion of the transition radiation (OTR). The OTR is imaged onto cooled CCD cameras to measure the transverse profile of the electron bunch ≈1 m upstream and down-stream of the plasma. The upstream OTR image provides information about the beam size and transverse profile coming into the plasma while the downstream OTR measures plasma focusing and deflection of the beam. All transition radiators are 1 μm thick titanium foils.

Retrieval of the bunch current profile

The achievable electric fields in the plasma depend strongly on the bunch length (or peak current profile), and the amount of charge that is accelerated depends on the electron population in the back of the bunch. However, for bunch lengths in the order of 100 fs, a streak camera does not provide sufficient resolution to measure the longitudinal structure. While the CTR Michelson interferometer can be used to measure the bunch length, it is both an average and symmetric measurement that cannot yield detailed information on the bunch current profile. Therefore, a different method had to be found to infer the longitudinal bunch shape from other information. The numerical code LiTrack models the development of the longitudinal phase space in the linear accelerator and is therefore used to predict the current distribution and energy spectrum of the bunch for a given setting of the relative phases and momentum compaction factors in the accelerator. However, there are no direct measurements of all the factors, which affect the compression with sufficient accuracy. By comparing the energy spectra that have been measured on the X-ray spectrometer to the ones obtained from the simulation, the accelerator set- tings can be reconstructed on a shot-by-shot basis and the longitudinal profiles can be inferred.

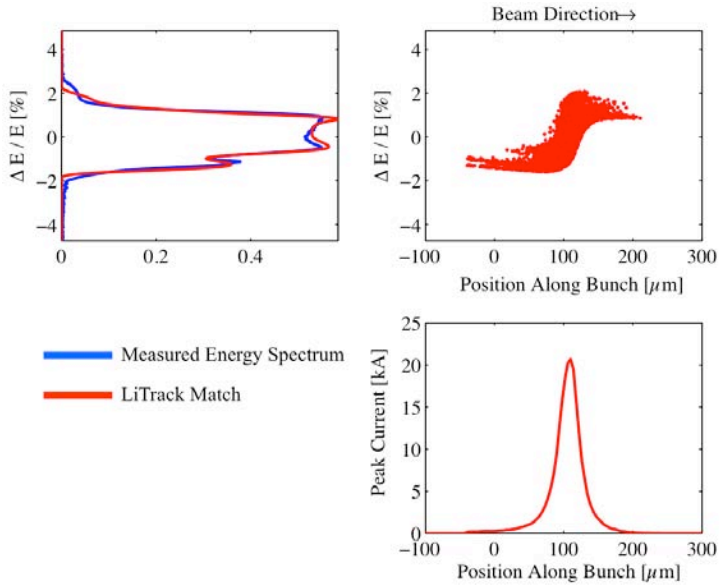

Figure 16: An example of the beam energy spectrum measured for a single event (blue) and the calculated LiTrack match (red) are plotted in the upper left. The resulting longitudinal phase space (upper right) and the inferred current profile (lower right) are also shown.

Beam energy spectrum after the plasma, Cherenkov radiator

In the history of the plasma experiments in the FFTB, two different approaches were employed to measure the energy spectrum of the beam exiting the plasma. The first used quadrupole and dipole magnets to form an imaging magnetic spectrometer. This technique works well in regimes were the energy spread imparted to the beam is relatively small. The second technique uses a strong dipole magnet to disperse the beam immediately after the plasma. The beam profile in the dispersive plane is measured at two locations downstream of the dipole to differentiate changes in energy from transverse deflections – see Figure 17. SABER will reconstitute both of these energy measurement capabilities.

The quadrupoles downstream of the SABER focal point will, in conjunction with the dipole dump magnet, form the magnetic imaging energy spectrometer. The spectrometer images the beam exiting the plasma onto a piece of aerogel in an energy dispersive plane. The visible Cherenkov radiation from the aerogel is imaged onto a cooled CCD camera with 16-bits of dynamic range. The electron bunch vertical profile is dominated by the vertical dispersion and is the energy spectrum. Imaging the beam mitigates the strong plasma focusing and deflecting forces. The transverse profile in the dispersive plane is then an unambiguous measurement of the energy spectrum of the bunch exiting the plasma. Thus without the plasma, the current distributions obtained from the Cherenkov images, spectra can be calibrated against the X-ray chicane (Figure 13) result. Then when the beam forms and interacts with the plasma, the x-ray chicane image gives us the input beam energy spectrum while the Cherenkov image (in the dispersive plane) gives us the effect of the plasma on the beam energy spectrum and on the beam transverse size (in the non-dispersive plane). This technique is optimum when the energy spectrum exiting the plasma is less than 10% wide. When the energy spread becomes too large, the quadrupoles providing the imaging condition over focus the low energy particles resulting in the distributed loss of these particles into the beam pipe.

To measure the energy spectrum in the regime with large energy spreads (~200%), experiment E-167 used the set-up shown schematically in Figure 17. A similar setup will be implemented in SABER.

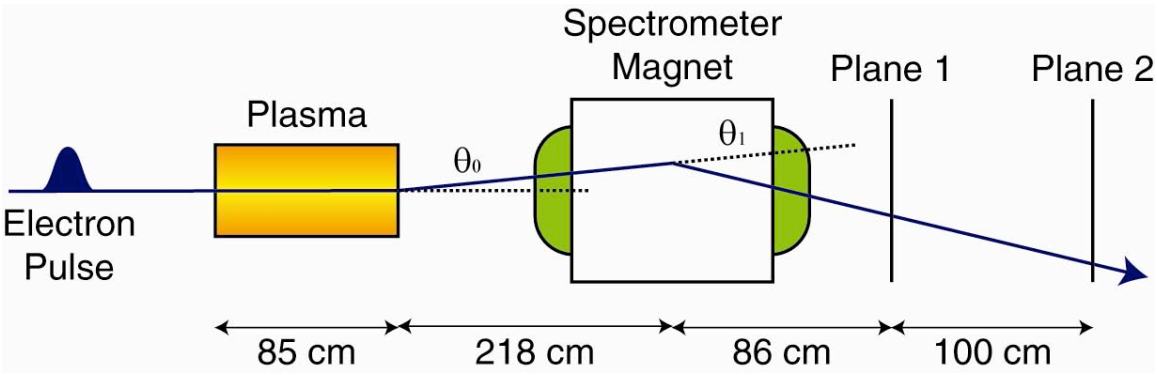

Figure 17: Schematic of the large energy spread spectrometer. Two cameras record the energy-dispersed images at Planes 1 and 2. A combination of low dispersion at Plane 1 and a lower lens magnification on the camera allows a broad energy spectrum of the beam including energy gain and loss to be recorded. A higher dispersion at Plane 2 coupled with a larger lens magnification is used to record images showing greater detail of the energy gain. The comparison of these two images allows for an independent measurement of vertical deflection and energy gain.

Plasma light diagnostics

In this single bunch experiment most of the energy lost by the bunch particles remains in the wake fields and is eventually dissipated in the plasma. A fraction of this energy is emitted in the form of atomic radiation from the excited plasma ions and recombined neutrals. Examining the spectrum of the light emitted by the plasma therefore leads information both on which atomic species is ionized and excited and in a relative sense, of how much energy is deposited in the plasma. This diagnostic therefore provides an independent monitoring of the plasma wake amplitude. It also provides information about possible ionization of the second lithium electron and of the oven helium buffer gas. These ionization processes are possible source for the trapped particles observed in the experiment (see section 3.2). Appearance of these particles also coincides with the abrupt increase in the amount of light collected downstream of the plasma. The increase in total charge in is on the order of that in the beam. The relative amount of light increase is up to several orders of magnitude larger than the relative charge increase and is the result of the coherent emission of light by short temporal structures of the trapped particles. Analysis of the beating structure in the measured visible light spectra is direct evidence that there is more than one distinct bunch. An example of the measured visible

spectrum emitted from the trapped particles is shown in the top of Figure 18. The beating structure in this image agrees with trapped particles following the primary bunch by ~70μm, in good agreement with the calculated plasma wavelength of 64μm. The bottom of Figure 18 shows the output of an OSIRIS simulation indicating that He electrons are trapped and bunched in a short (2μm long) region near the peak-accelerating field of the first wake bucket.

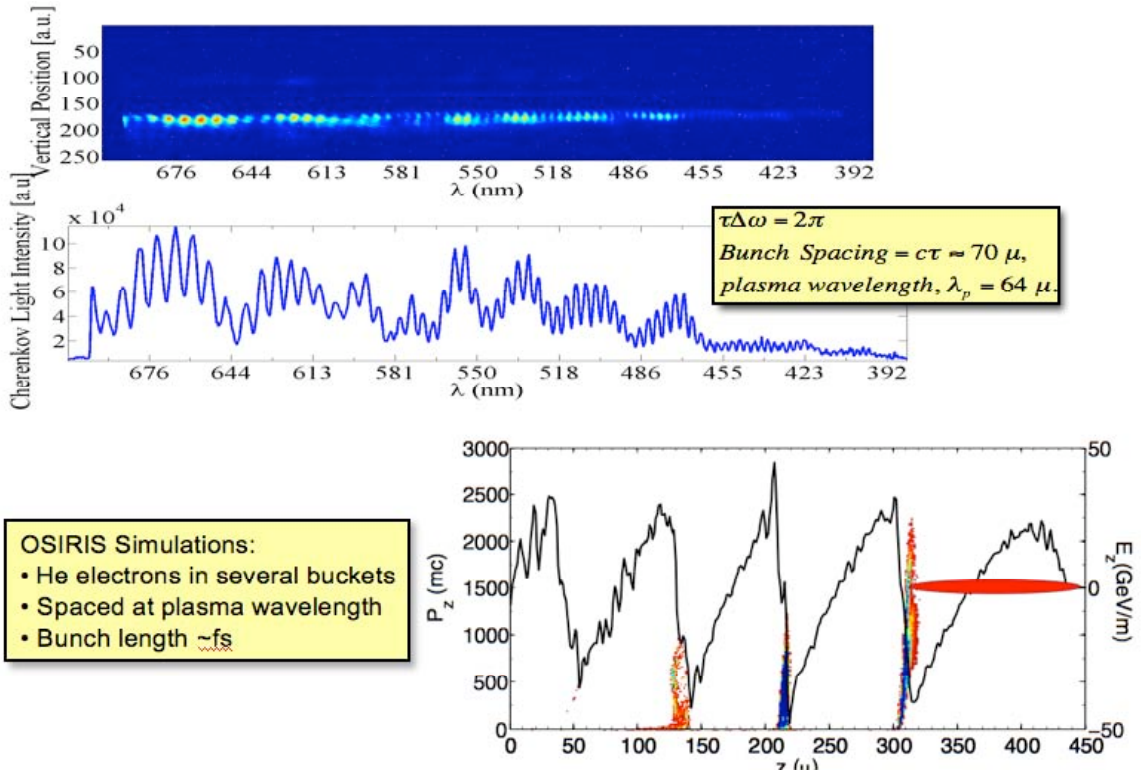

Figure 18: (Top) A portion of the visible light spectrum measured downstream of the plasma and the resulting beating pattern resulting from the second bunch of trapped particles. (Bottom) OSIRIS computer simulation indicating trapping of short bunches of helium electrons in the spikes of the lithium plasma wake.

Cherenkov Cell Diagnostics

Downstream of the plasma, the beam passes through a small dipole, $\int B \cdot dl = 0.033$ Tm, and then a cell filled with up to an atmosphere of helium gas. The beam emits Cherenkov radiation as it passes through the cell, and a titanium foil acts as a mirror to reflect out the light. The far-field of this light is imaged with an optical camera, and the spectrum is collected with a spectrograph. Since, for a fixed momentum, the

Cherenkov light is emitted with a delta function in angle, the electrons show up as rings on the camera. The dispersion from the magnet makes different energy electrons show up as rings with different displacements. The energy of the trapped electrons is determined from the displacements of the rings, and temporal information is found from the intensity and spectrum of the Cherenkov light.

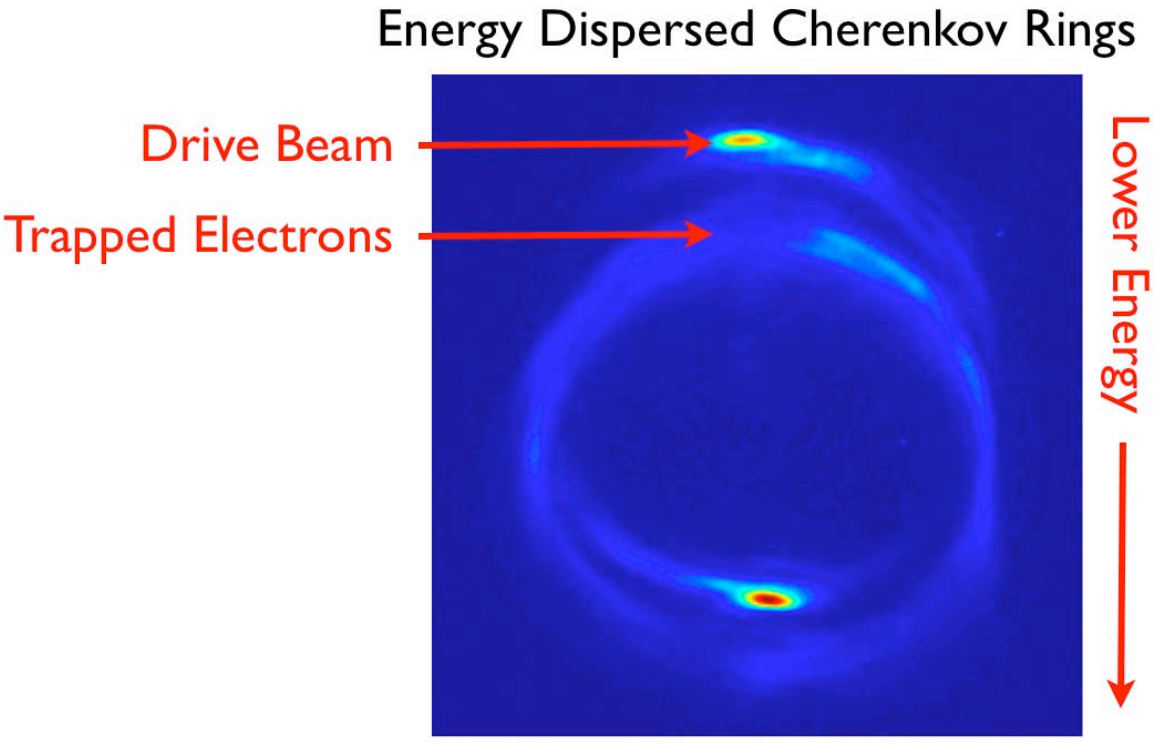

Figure 19: Images of the Cherenkov light cones emitted by the drive beam and trapped particles passing through a gas cell after the plasma (see Figure 8).

Data acquisition and handling

A distributed computer system has been set up to acquire the large amount of data generated by the experiments. For each bunch, up to five images are stored in addition to the values that the SLC Control Program (SCP) records. For each day of the run, an average of 7.5 GB of data is accumulated.

5 Experimental program schedule

We anticipate there will be work early in calendar year 2007 to help commission the SABER beam. Our collaboration has unique experience with optical diagnostics that

we hope to iterate and improve at SABER. Specifically, we will continue our work with interferometery to characterize the bunch compression and implement Optical Transition Radiation (OTR) and Optical Diffraction Radiation (a.k.a. ODR == OTR with no foil, just an aperture) for 10Hz tuning and single shot emittance measurements.

Following successful commissioning of the beam we can begin the plasma-based experiments described in this proposal. In the FFTB three weeks was a good duration for a single run and this is a good estimate for what we will need at SABER. The running for the upcoming year is linked to LCLS commissioning. Successful completion of the proposed experiments will require a minimum of two three-week long runs.

6 Summary

Over the past seven years, this collaboration performed a series of experiments that have yielded a number of rich new beam and plasma physics results, demonstrated the promise of beam-driven plasma accelerators and developed a sophisticated laboratory infrastructure for beam and plasma experiments in the Final Focus Test Beam (FFTB). The FFTB was decommissioned in April 2006 to make way for the Linac Coherent Light Source (LCLS). For the experiments proposed here we will relocate much of this infrastructure to the South Arc Beamline Experimental Region (SABER).

This proposal aims to explore the physics questions beyond energy doubling: What is the maximum energy gain achievable – can the energy be more than doubled? How much of the beam energy can be transferred to the plasma wake? Do instabilities become important over long plasma lengths and in the presence of large energy loss? Additionally, the >30GeV/m accelerating gradients demonstrated in E-164X and E-167 revealed a new physical phenomena where plasma electrons are trapped in the plasma wake and exit the plasma. Initial measurements hint that these self-injected particles have many intriguing features making them potentially interesting in their own right: pulse durations of 10's of fs and an emittance smaller than the bunch producing the plasma wake. Studying the trapping mechanism and the resulting bunch properties will be an integral part of our work.

These experiments are based largely on existing apparatus and on the experimental techniques developed over the years in the FFTB. During the

commissioning phase of SABER, we will implement new and improved diagnostics that will allow for a better measurement of the beam current distribution to further our understanding the processes in the plasma. We will thus expand and upgrade our optical transition radiation (OTR) monitors to allow for single shot, non-destructive emittance measurements and to aid beamline set-up and commissioning. Once beam parameters similar to those used in the FFTB will be established in SABER and our experimental apparatus will be relocated, our program will begin in earnest.

We anticipate this proposal will be the first in a series, beginning a second chapter of a long-term program studying beam-plasma interactions at SLAC. Future proposals will aim to exploit the upgraded capabilities proposed for the SABER completed facility – operational independence from LCLS and for the first time, compressed positrons.

Appendices

A. Highlights of the Experiments

E-157:

Collective Refraction of the Electron Beam at a Plasma-Gas Interface

P. Muggli et al., Nature, Vol. 411, p. 43 (2001),
P. Muggli et al., Phys. Rev. Special Topic-AB Vol. 4, 091301 (2001)

The observation of refraction and eventual total internal reflection of the electron beam as it exits the plasma/gas boundary was among the unanticipated results of E-157. The interface is produced by a well-defined laser beam, which is used to create the plasma via photo-ionization of a column of lithium vapor. The observed refraction is analogous to the usual refraction for a light beam, however the associated "Snell's law" is time-dependent and non-linear.

A physical explanation for this effect is as follows. In the plasma, the electron beam, with density greater than plasma density, has a symmetric focusing force on it because of the expulsion of plasma electrons. However, as the beam begins to exit the plasma the focusing force becomes a deflecting force, bending the beam away from its trajectory toward the plasma. This deflection has been measured as a function of the incoming beam angle and found to be in quantitative agreement (see Figure A.1) with both a model and three-dimensional PIC code simulations of the experiment.

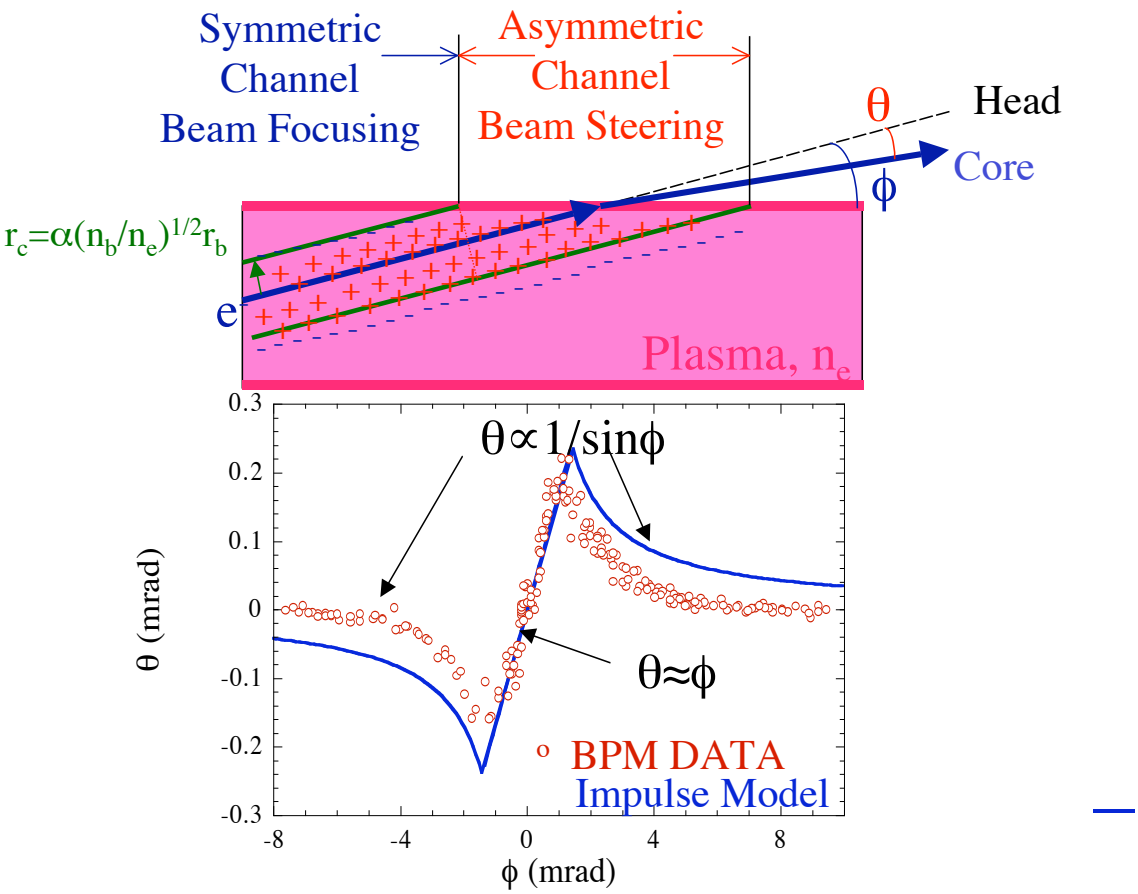

Figure A.1: Cartoon (top) showing the physical reason for refraction of an electron beam at the plasma/gas boundary and the observed angle of refraction as a function of the incident angle ϕ.

Transverse Betatron Dynamics of a 30 GeV Beam in a Long Plasma

C. Clayton et al., Physical Review Letters, Vol. 88, 154801 (2002).

In the E-157 experiment, the electron beam was not "matched" to the plasma. Consequently, the betatron motion of individual electrons produces multiple oscillations of the electron beam envelope over the plasma length. Thus, the spot size of the electron beam on a screen downstream of the plasma oscillates as the plasma density is increased. In Figure A.2, we show these oscillations measured during E-157 experiment. The solid line is the prediction of a model based on the focusing force on the beam provided by a uniform ion channel. The model has no free parameters. One can see that this model predicts both the densities where a minimum spot size is expected and the amplitude of the oscillations rather well. At the highest densities, there is a breakdown of the model as the plasma density becomes comparable to the beam density and the beam is unable to completely blow out the plasma electrons and establish the ion channel.

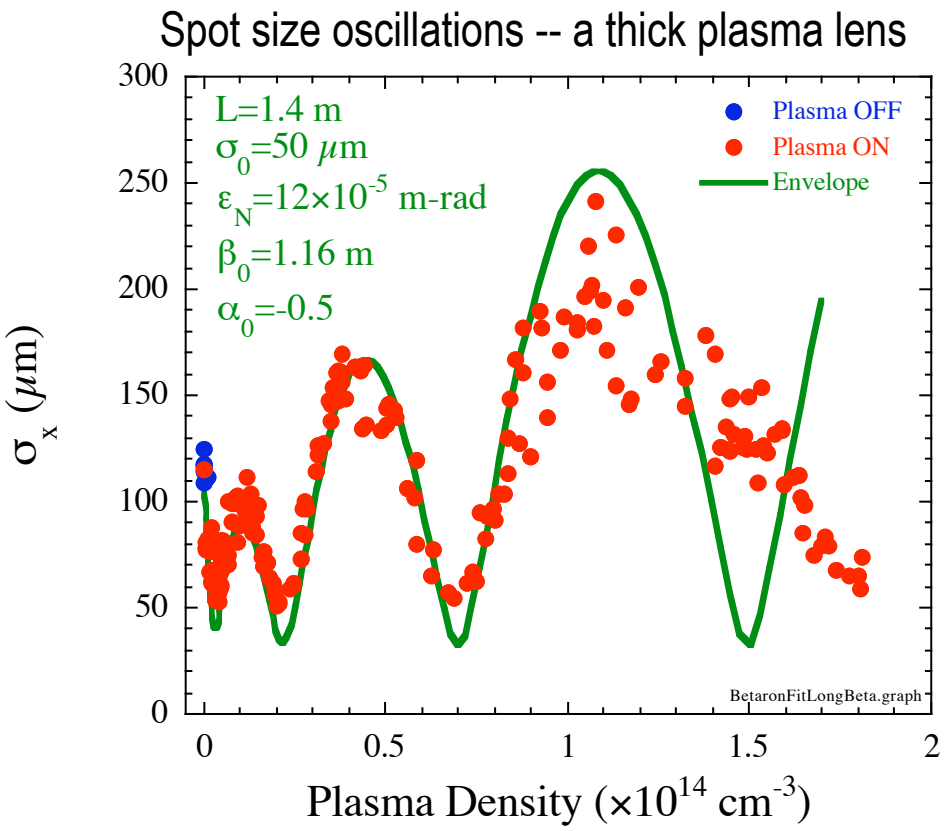

Figure A.2: The observed variation of the electron beam spot size on an external screen as the plasma density is increased in the E-157 experiment.

Demonstration of a Plasma Wiggler with High Beam Brightness

S. Wang et al., Physical Review Letters, Vol. 88, 135004 (2002).

The betatron oscillation of the beam envelope by the transverse electric field of an ion column results in the generation of synchrotron radiation. Since the beam at SLAC is ultra-relativistic, this emission is strongly peaked in the forward direction. Even though the emission is incoherent and broadband, the peak brightness of the x-ray beam is comparable to the undulator radiation at synchrotron light sources.

In the E-157 experiment, we measured the absolute photon yield, the angular spread and the density dependence of the X-rays. The X-rays were emitted with a divergence angle of 0.1-0.3 mrad, and the x-ray yield varied quadratically with plasma density. The absolute photon yield and the peak spectral brightness at 14.2 keV were estimated to be $6 \cdot 10^{5}$ and $7 \cdot 10^{18}$ per (second mrad^2 mm^2 0.1% bandwidth). Figure A.3 shows an image of the X-rays on a fluorescent screen placed 40 m downstream of the plasma in the E-157 experiment. A well-defined beam due to betatron x-rays is clearly visible on top of the bending magnet radiation generated as the 30 GeV electron beam is swept out of the way.

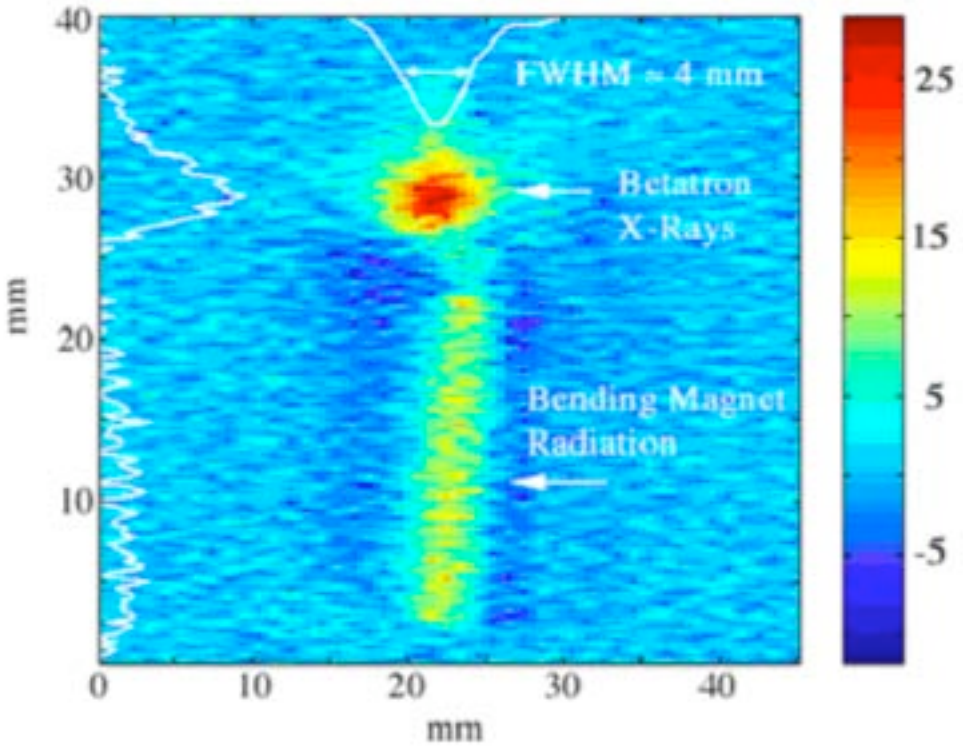

Figure A.3: Betatron radiation emission of X-rays above 6 keV seen in the E-157 experiment.

E-162:

Focusing of a Positron Beam

M. Hogan et al., Physical Review Letters, Vol. 90, 205002 (2003).

The mechanism for focusing of a positron beam by a plasma is quite different than that of an otherwise identical electron beam. In the case of a positron beam, the plasma electrons are sucked in from different radii outside of the beam. These electrons arrive at different times and the peak electron density on axis of the positron beam can far exceed the beam density. Thus the focusing force is neither linear in the radial direction nor is it constant in the longitudinal direction as it is in the electron beam case in the "blowout" regime.

We have measured both the time-integrated and time-resolved focusing of the SLAC positron beam as it traverses a 1.4 m long plasma column. The time-integrated measurement was done by measuring the beam size at two different locations downstream of the plasma as a function of plasma density. A maximum demagnification of a factor of two has been demonstrated (see Figure A.4)

The time dependent focusing of the beam has been measured using a streak camera and compared with simulations using the code QUICKPIC. The focusing force is seen to vary in a nonlinear fashion along the full 12 ps length of the positron beam.

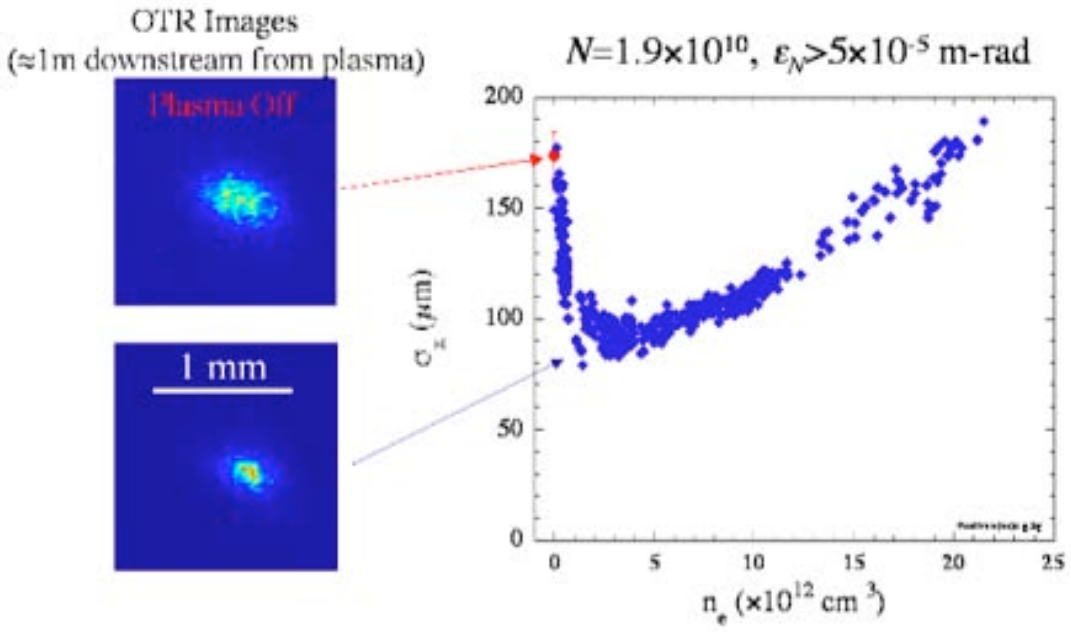

Figure A.4: Focusing of the 28.5 GeV positron beam. The spot size of the positron beam measured on a screen placed approximately 1 m after the plasma as a function of plasma density.

Dynamic Focusing Within a Single Ultra-Relativistic Electron Bunch

C. O'Connell et al., Phys. Rev. Special Topics-AB, Vol. 5, 121301 (2002).

In the blow-out regime, as the beam propagates through the plasma, the density of plasma electrons along the incoming bunch drops from the ambient density to zero leaving a pure ion channel for the bulk of the beam. Thus, from the head of the beam up to the point where all plasma electrons are blown out, each successive longitudinal slice of the bunch experiences an increasing focusing force due to the plasma ions. The time-changing focusing force results in a different number of betatron oscillations for each slice depending upon its location within the bunch. Since the incoming electron beam has a correlated energy spread, this time-dependent focusing of the electron bunch has been observed by measuring the beam spot size at the Čerenkov radiator, which is in the image plane of a magnetic energy-spectrometer imaging the plasma exit. Each plot in Figure A.5 represents a section in time, where time progresses from left to right, then top to bottom. We see that the number of betatron oscillations within the bunch increases towards the back of the bunch (Figures A.5a-g) but only up to the blowout time occurring approximately at the plot labeled $\tau = 0$ ps (Figure A.5h). Clearly, each successive slice of the bunch, from $\tau = -4.9$ ps to $\tau = 0$, is experiencing a stronger effective focusing force than the slice prior to it. Conversely, the ambient plasma density needed to reach any given minimum decreases with time along the bunch. The locations of the minima are both slice-and density-dependent. Figures A.5il are in the blow-out regime as the focusing force is no longer changing.

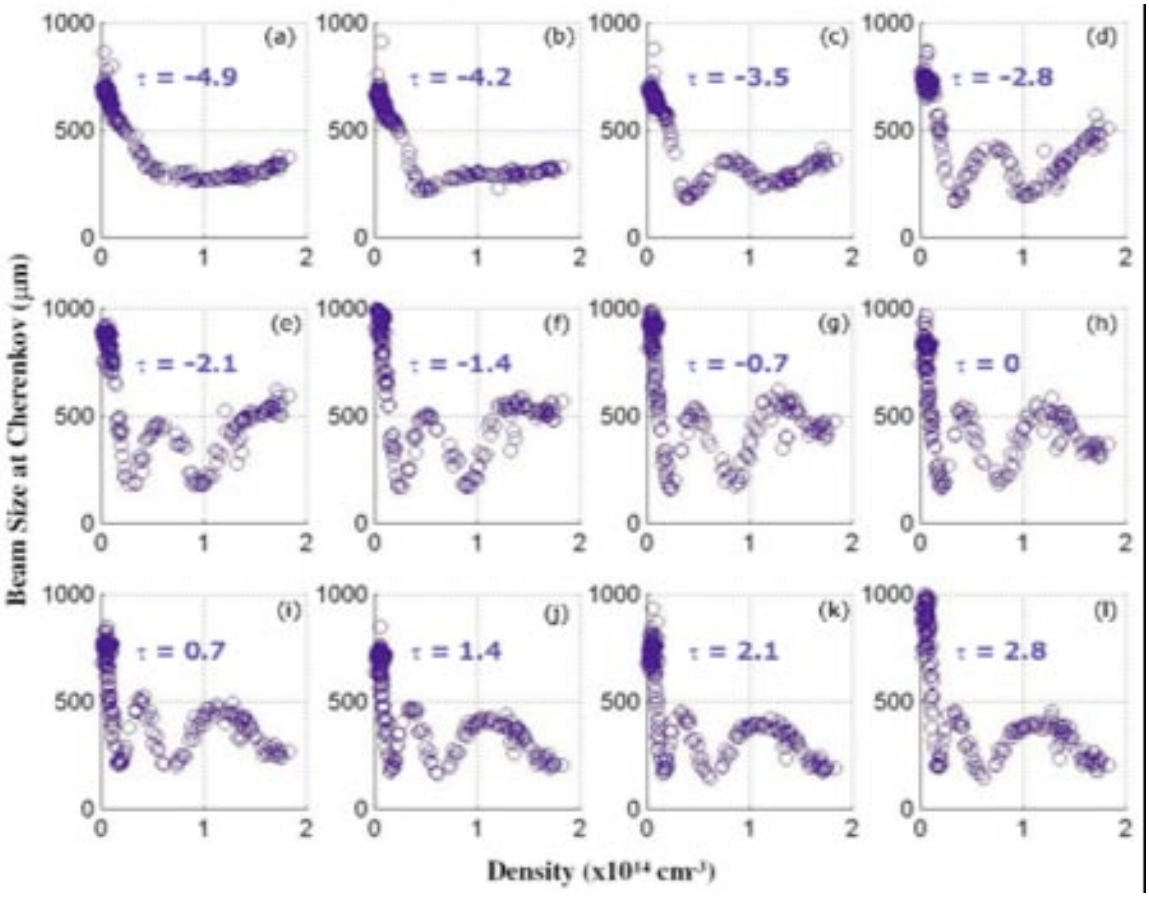

Figure A.5: Individual Čerenkov Time Slices (read L-R, T-B). Graph (a) shows the weak focusing force, which dominates the first head slice. Beginning at graph (b) the slices are in the linear portion of the chirp. Graphs (i)-(l) are in the blowout regime, since the focusing force is no longer changing.

Acceleration of Positrons by the Plasma Wakefield

B. E. Blue et al., Physical Review Letters, Vol. 90, 214801 (2003).

High-gradient acceleration of both positrons and electrons is a prerequisite condition to the successful development of a plasma-based e^+-e^- linear collider. Such an accelerator employs the longitudinal electric field of a relativistically propagating wakefield in a plasma to accelerate charged particles. In proof-of-principle experiments, laser-driven plasma wakefields have been shown to accelerate electrons at electric fields that are significantly greater than those employed in current radio-frequency accelerators are. We have now shown for the first time that a beam of positrons can drive and be used to probe the longitudinal electric field component of the plasma wakefield. When a 28.5 GeV, 2.4 ps long positron beam at the Stanford Linear Accelerator Center containing $1.2 \cdot 10^{10}$ particles propagates through a Lithium plasma of electron density $1.8 \cdot 10^{14}$ cm^{-3}, the main body of the beam is decelerated at a rate of approximately 49 MeV/m, while a beam slice containing $5 \cdot 10^{8}$ positrons in the back of the same bunch gains energy at an average rate of ~ 56 MeV/m over 1.4 m. These results are critical to the development of future plasma based linear colliders. Figure A.6 shows the summary of results on positron acceleration from a paper published in Physical Review Letters.

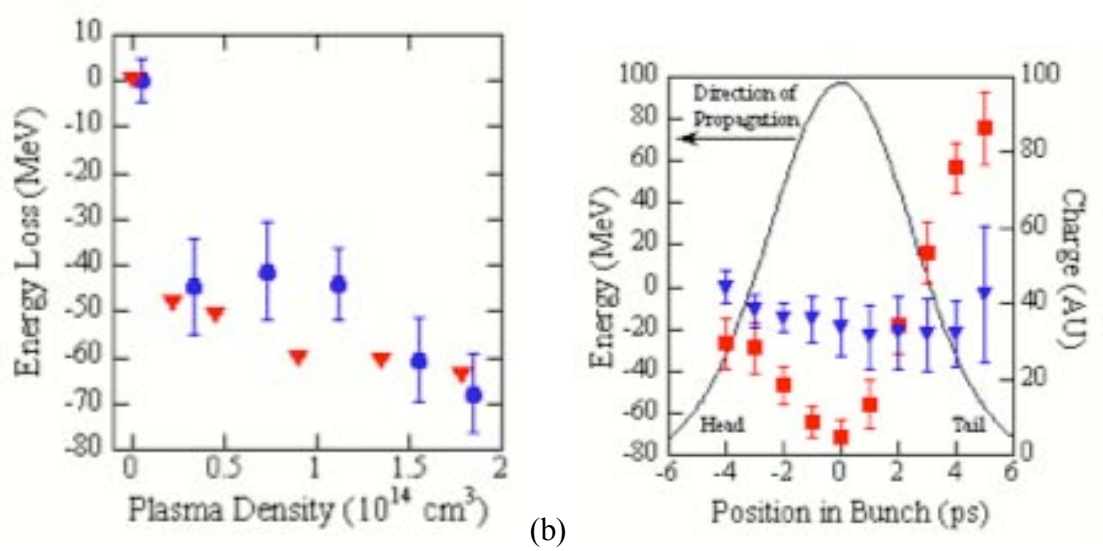

(a) (b)

Figure A.6: (a) The energy loss by the center 1 ps slice of the positron beam as a function of plasma density (blue circles) and the prediction from 3D, OSIRIS simulations. (b) The slice-by-slice energy change of the positron beam showing both energy loss in the front half and the energy gain in the back half of the beam for a density of $1.5 \cdot 10^{14}$ cm^{-3}. The red curve is with the plasma on and the blue curve is with the plasma off. The black curve is the positron beam charge distribution.

Electron Beam Acceleration Using a Matched Beam in a Plasma

P. Muggli et al., Physical Review Letters, Vol. 93, 014802 (2004).

The key to control the transverse effects of the plasma was to propagate a matched beam. In a matched beam the emittance force of the beam balances the focusing force by the plasma and the beam propagates without spreading, i.e., it exits the plasma as it entered it, which makes it easy to image the beam. Figure A.7 shows conclusive evidence for matched-beam propagation. At lower densities, the emittance force of the beam exceeds the focusing force. As the focusing force is increased (by increasing the density), the beam spot size oscillations damp down. Eventually the beam is matched to the plasma.

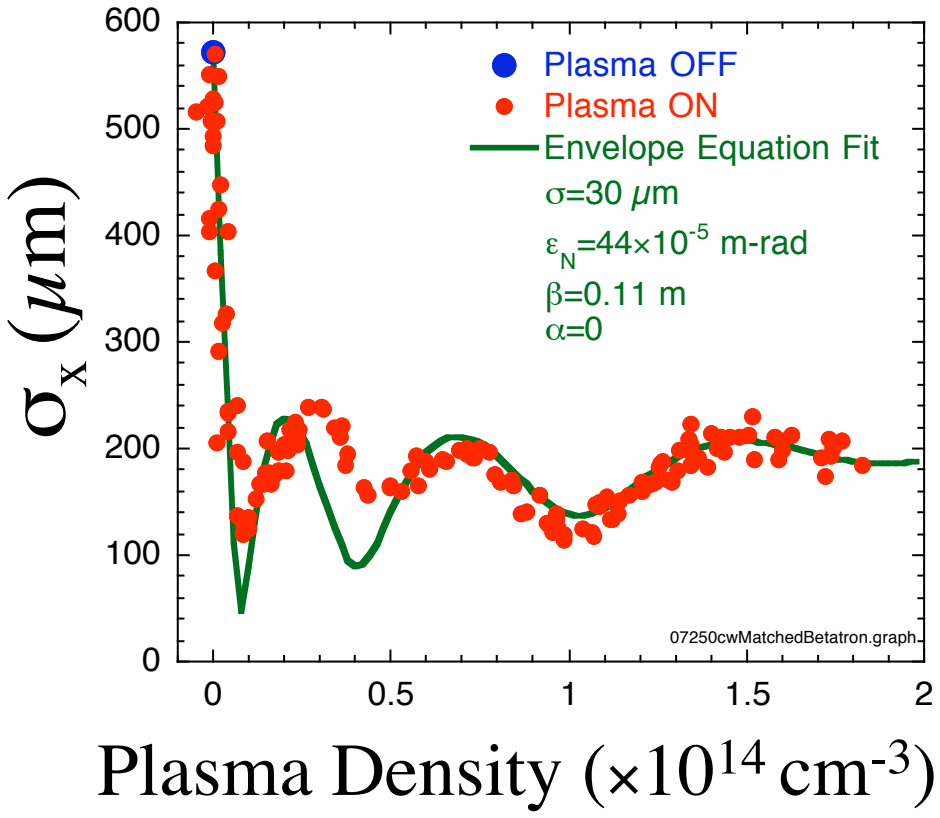

Figure A.7: Variation of the transverse spot size of the beam vs. plasma density. Initially the beam emittance force is larger than the plasma focusing force. As the two forces become equal the beam spot oscillations damp out and the bean is said to be "matched."

A breakthrough, which produced unambiquous results, was the conversion of the dispersion (dipole) magnet into a proper imaging spectrometer. This together with a streak camera to time resolve the dispersed images of the beam lead to clear evidence for energy loss of the bulk of the beam followed by energy gain of the latter slices of the beam.

Figure A.8 shows the change in energy of the picosecond wide slices of the beam. The peak energy loss and gain were about 160 MeV for a density of 1.8×10^{14} cm^{-3}. However, this number is for the centroid of the slice. The maximum energy gain was ~ 275 MeV in good agreement with 3D PIC code simulations of our experiment.

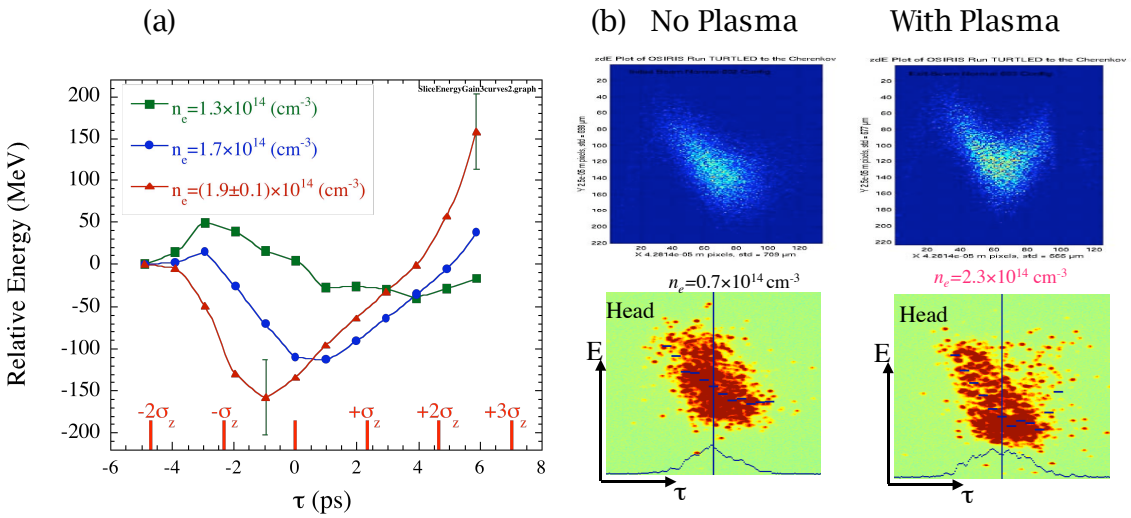

Figure A.8: (a) Relative change in energy of 1 ps wide slices of the beam at three different densities. At the highest density, energy loss of most of the beam slices and energy gain by the last two beam slices can clearly be seen. (b) PIC code simulations and corresponding streak camera data of energy dispersed slices of the beam without and with the plasma (E-162 experiment).

Halo Formation Around Positron Beam Core

P. Muggli et al., to be submitted for publication

The understanding of how intense, ultra-relativistic electron and positron beams propagate through meter-scale, dense plasmas critical to the development of a beam-driven, plasma wakefield accelerator. In particular, any physical effect that can degrade the transverse emittance of the beam as it traverses the plasma is deleterious to the final luminosity that can be achieved in this scheme. For instance, the extremely nonlinear transverse wakefields induced in the plasma by a positron beam can increase the slice emittance of the beam. This manifests itself by forming a halo around the core of the positron beam. Although much work has been done on understanding how beam halos are formed in space-charge dominated electron and ion beams, there is not work done on halo formation around an ultra-relativistic positron beam. In this case, it is the nonlinear focusing forces and not the space charge that is responsible for the loss of beam particles from the core to the halo.

As part of E-162 we carried out the first experimental and numerical study of halo formation in a high charge (3 nC), ultra-relativistic (28.5 GeV) positron beam after propagating through a 1.4 m long, dense ($n_e \quad 5 \cdot 10^{14}$ cm^{-3}) plasma column. This is done by analyzing the images of the beam before and after the plasma. The beam entering the plasma has an emittance ratio ($\varepsilon_x/\varepsilon_y$) of 5. As the plasma density is increased, the core of the beam exiting the plasma is seen to be nearly symmetric with more and more particles contributing to the halo that surrounds this core. Simulations of the experiment using a particle-in-cell code give a good agreement on both the beam spot-size and the fraction of particles in the core with the experimental measurements. Simulations indicate that the slice emittance of the beam increases along the bunch and that an incoming beam with grossly unequal emittances, exits the plasma with approximately equal emittances in both transverse planes. This is clearly seen in Figure A.9. This self-matching of the beam to the plasma through emittance growth is a characteristic particular to positron beams.

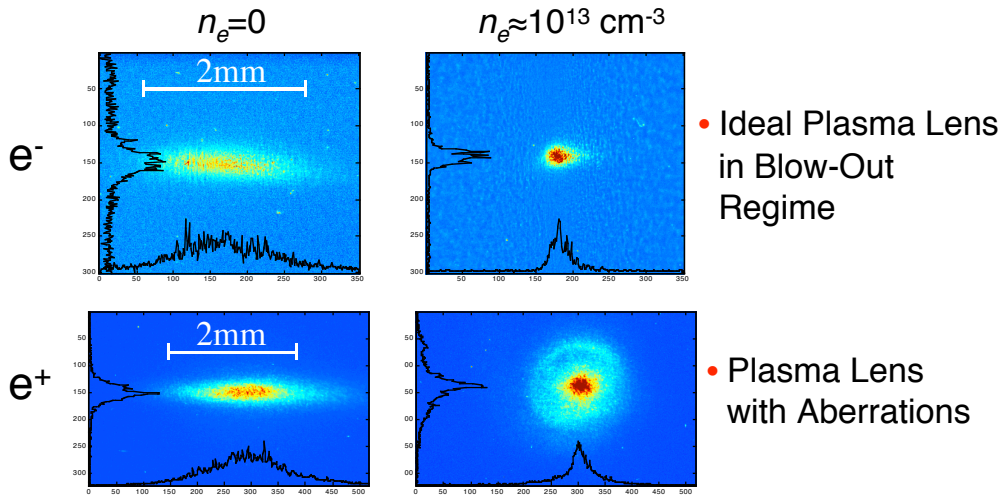

Figure A.9: The difference between focusing of grossly asymmetric ultra-relativisitic electron and positron beams by an underdense plasma lens. The electron beam shows a clear tightly focused spot while the positron beam displays a focused core surrounded by a halo indicative of an aberrated lens.

E-164/E-164X:

Plasma Production Via Field Ionization

C. O'Connell et al. Phys. Rev. STAB 9, 101301 (2006)

The original idea of E-164 was to increase the average gradient of the PWFA from 100 MeV/m (seen in E-162) to 5 GeV/m by reducing the pulse length from 700μm to 100 μm. It was pointed out by Dr. Bruhwiler at the Advanced Accelerator Conference 2002 that as the beam became shorter the transverse electric field of the beam itself would eventually field-ionize the atoms and produce a plasma. Furthermore, the transverse size of the plasma can be larger than the beam.

In Run 1 of E-164, this field ionization became apparent for the first time. At a charge of $N = 1.2 \cdot 10^{10}$, σ_z = 100 μm and σ_r = 20 μm, the beam modified the plasma density via field-ionization (also called tunnel-ionization) at the peak of the beam (see Figure A.10). However, because we were at the threshold for field-ionization, the plasma formation was not very reproducible and in any case there were not too many beam particles left in the back of the beam to "see" the accelerating phase of the wake. It was decided therefore to go to even shorter bunches in E-164 Run II to increase the electric field associated with the beam.

We have taken an extensive amount of data on field ionization of H_2, He, NO and Li by varying the beam charge, beam spot size, and the pulse width. The diagnostic of the onset of the plasma formation is the sudden onset of energy loss experienced by the main body of the beam whereas the diagnostic of formation of a fully ionized plasma is the eventual saturation of this energy loss at some maximum value.

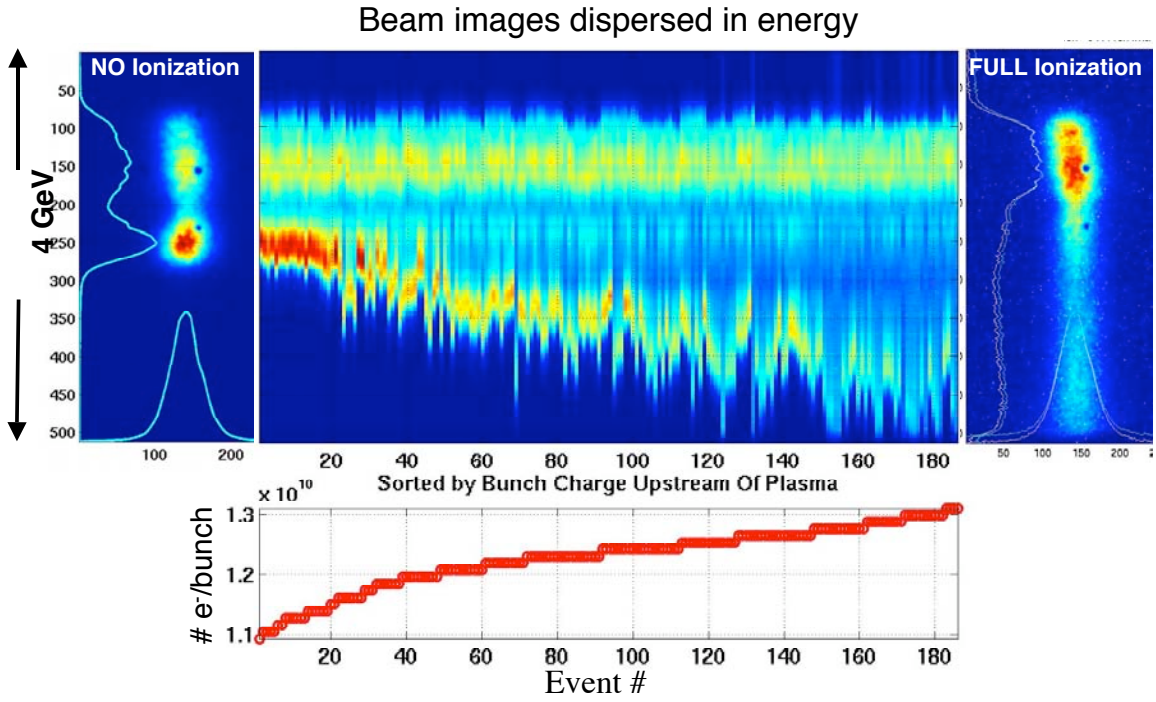

Figure A.10: The change in beam energy as a function of beam charge in the E-164 Run I. Up to 1.2 x 10^{10} electrons the beam energy spectrum shows only a slight change. For a charge greater than 1.2 x 10^{10} the electric field of the beam ionizes the Li and produces a fully ionized plasma. A wake response leads to the beam suddenly losing more than 1 GeV energy.

Observation of Greater Than 3 GeV Energy Gain

M. J. Hogan et al., Phys. Rev. Lett. 95, 054802 (2005)

E-164X has demonstrated energy gain of more than 1 GeV in a 10 cm long plasma. This is both the largest energy gain ever achieved by a plasma accelerator and the largest accelerating gradient ever achieved by a beam driven plasma wakefield accelerator. The results were made possible by the combination of short electron bunches (~30 μm or 100 fs) and field ionized plasmas in the $3 \cdot 10^{17}$ cm^{-3} density range.

In previous experiments where the bunches were > 1ps the energy changes imparted by the plasma wakefield were of the same order or smaller than the incoming energy spread. To directly measure the effects of the plasma wakefield we used a streak camera to time resolve the energy spectrum and compare plasma on and off events (**Figure A.8**).

With the 100 fs bunches in E-164X it is no longer possible to time resolve the energy spectrum and the energy changes imparted by the plasma must be larger than the 1.2 GeV (full width) energy spread of the incoming bunch. Longitudinal wakefields in the main linac impose an additional challenge by giving the particles in the back of the bunch (which we accelerate) the lowest incoming energy. Thus, particles in the back of the bunch must be accelerated by more than 1.2 GeV before energy gain can be observed. **Figure A.11** shows the energy spectrum for two similar bunches with and without the 10 cm long $2.7 \cdot 10^{17}$ cm^{-3} plasma.

Typically about 7% of the incoming $2 \cdot 10^{10}$ electrons are accelerated to energies greater than the maximum incoming energy, with some particles gaining more than 3 GeV. We have observed many such events and the acceleration signal is consistent and reproducible.

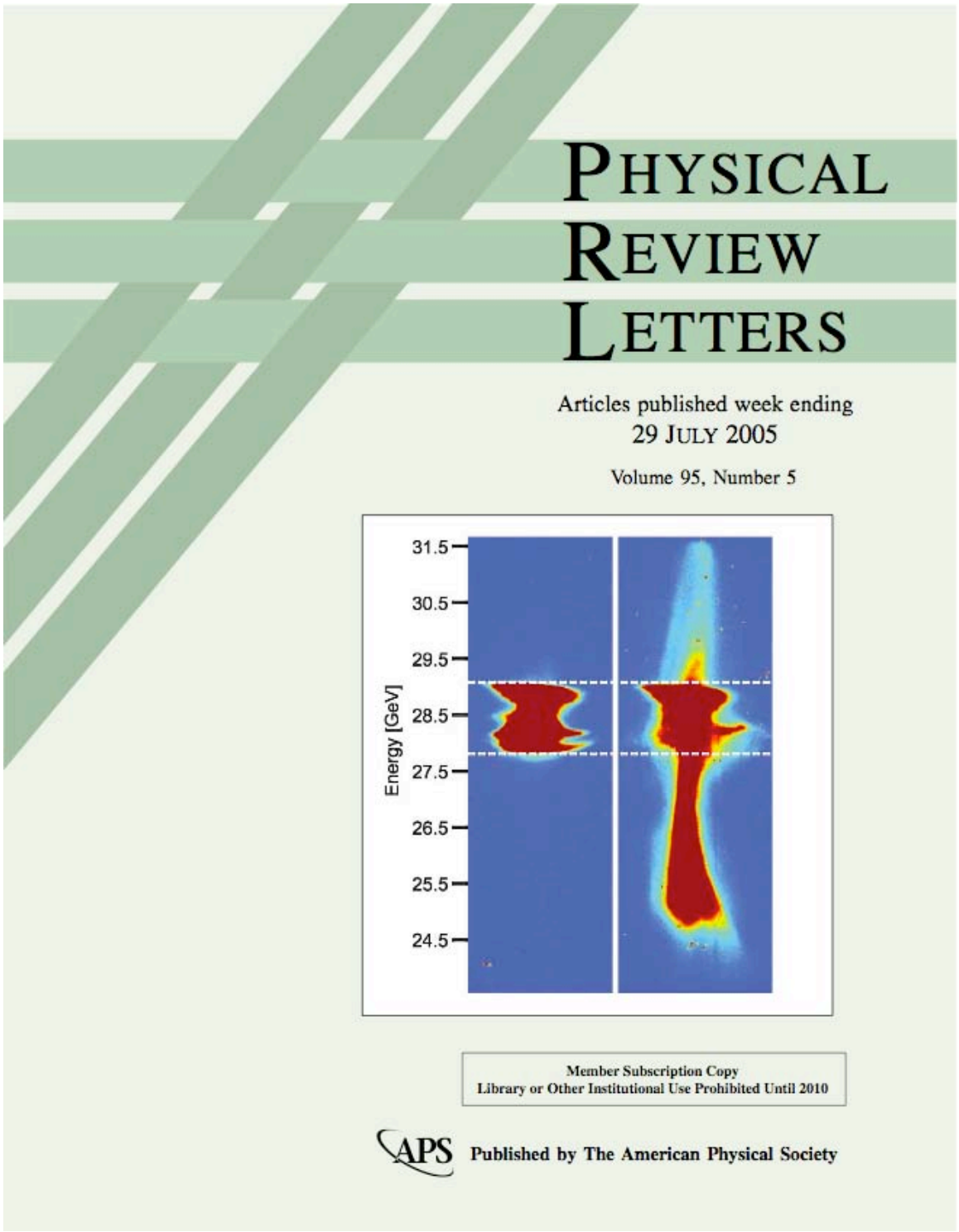

Figure A.11: The energy spectrum of the nominally 35μm long electron beam without the plasma and after it traverses the 10 cm long plasma. The beam has an approximately 1.5GeV head-to-tail energy spread. With the plasma on, one can clearly see energy loss of the bulk of the beam and energy gain of the tail particles in the beam.

E-167:

Energy Doubling of 42GeV Electrons in a Meter-scale Plasma Wakefield Accelerator

I. Blumenfeld et al., Submitted for publication 2006

E-167 showed more than 42 GeV energy gain in an 85 cm long plasma wakefield accelerator driven by a 42 GeV electron drive beam at the Stanford Linear Accelerator Center (SLAC). The results are in excellent agreement with the predictions of three-dimensional particle-in-cell simulations. Most of the beam electrons lose energy to the plasma wave, but some electrons in the back of the same beam pulse are accelerated with a field of ~52 GV/m. This effectively doubles their energy, producing the energy gain of the 3 km long SLAC accelerator in less than a meter. This experiment is a milestone in high-gradient accelerator research and is an important step toward demonstrating the viability of plasma accelerators for high-energy physics applications.

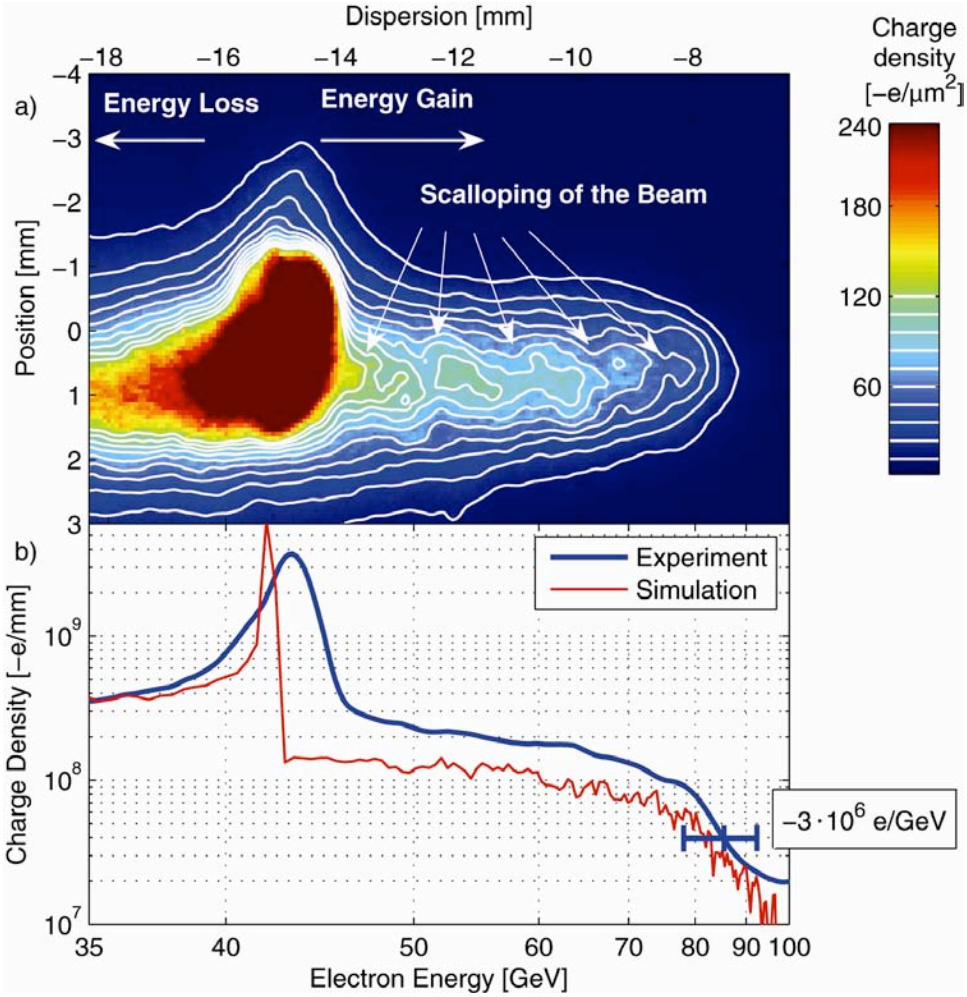

Figure A.12: a) Energy spectrum of the electrons in the 30-100 GeV. The image is shown with a colour map that saturates at −240 e/μm^2. The dispersion (shown on the top axis) is inversely proportional to the particle energy (shown on the bottom axis. The head of the pulse, which is unaffected by the plasma, appears at −15 mm, equivalent to 43 GeV. The core of the pulse, which has lost energy driving the plasma wake, is dispersed partly out of the field of view of the camera. Particles in the back of the bunch, which have reached energies up to 85 GeV, are visible to the right. The pulse envelope exits the plasma with an energy-dependent phase advance, which is consistent with the observed scalloping of the dispersed beam.(b) Projection of the image in Figure 2a, shown in blue. The simulated energy spectrum is shown in red. The differences between the measured and the simulated spectrum near 42 GeV are due to an initial correlated energy spread of 1.5 GeV not included in the simulations.

B. Publications

Peer-Reviewed Publications from E-157 / E-162 / E164 / E164X / E167

1) M. J. Hogan *et al, "*E-157: A 1.4 Meter-Long Plasma Wakefield Acceleration Experiment Using A 30 Gev Electron Beam From The Stanford Linear Accelerator Center Linac", Physics of Plasmas **7**, 2241 (2000).
2) P. Muggli *et al,* "Collective Refraction Of A Beam Of Electrons At A Plasma-Gas Interface", Nature **411**, 43 (3 May 2001)
3) P. Catravas *et al,* "Measurements Of Radiation Near An Atomic Spectral Line From The Interaction Of A 30 GeV Electron Beam And A Long Plasma", Physical Review E **64** 046502 (2001).
4) P. Muggli *et al*, "Collective Refraction Of A Beam Of Electrons At A Plasma-Gas Interface", Physical Review Special Topics - Accelerators and Beams **4**, 091301 (2001).
5) S. Lee *et al*, "Energy Doubler For A Linear Collider", Physical Review Special Topics - Accelerators and Beams **5**, 011001 (2002).
6) Shouqin Wang *et al,* "X-Ray Emission From Betatron Motion In A Plasma Wiggler", Physical Review Letters **88**, 135004 (2002)
7) C. E. Clayton *et al,* "Transverse Envelope Dynamics Of A 28.5 Gev Electron Beam In A Long Plasma", Physical Review Letters **88**, 154801 (2002)
8) C. Joshi *et al,* "High Energy Density Plasma Science With An Ultra-Relativistic Electron Beam", Physics of Plasmas **9**, 1845 (2002).
9) C. O'Connell *et al*, "Dynamic Focusing Of An Electron Beam Through A Long Plasma", Physical Review Special Topics – Accelerators and Beams **5**, 121301 (2002)

10) M. J. Hogan *et al*, "Ultrarelativistic-Positron-Beam Transport Through Meter-Scale Plasmas", Physical Review Letters **90**, 205002 (2003).

11) B. Blue *et al*, "Plasma Wakefield Acceleration Of An Intense Positron Beam", Physical Review Letters **90**, 214801 (2003).

12) C. Joshi and T. Katsouleas, "Plasma Accelerators At The Energy Frontier And On Tabletops", Physics Today, 47 (June 2003).

13) P. Muggli *et al*, "Meter-Scale Plasma-Wakefield Accelerator Driven By A Matched Electron Beam", Physical Review Letters **93**, 014802 (2004).

14) R. Maeda *et al*, "On The Possibility Of A Multi-Bunch Afterburner For Linear Colliders", Physical Review Special Topics – Accelerators and Beams **7**, 111301 (2004).

15) M. J. Hogan *et al*, "Multi-GeV Energy Gain In A Plasma-Wakefield Accelerator", Physical Review Letters **95**, 054802 (2005).

16) C.L. O'Connell *et al*, "Plasma Production via Field Ionization", Physical Review Special Topics – Accelerators and Beams **9**, 101301 (2006)

17) D. K. Johnson *et al*, "Positron Production by X-Rays Emitted by Betatron Motion in a Plasma Wiggler", Physical Review Letters **97**, 175003 (2006).

18) T. Katsoulaes, "Plasma accelerators race to 10 GeV and beyond", Physics of Plasmas Phys. Plasmas **13**, 055503 (2006).

19) Ian Blumenfeld *et al*, "Energy Doubling of 42 GeV Electrons in a Meter Scale Plasma Wakefield Accelerator", submitted to Nature

20) E. Oz *et al*, "Ionization Induced Electron Trapping in Ultra-relativistic Plasma Wakes", submitted to Physical Review Letters

Related Peer-Reviewed Simulation Papers

1) S. Lee *et al,* "Simulations Of A Meter-Long Plasma Wakefield Accelerator", Physical Review E **61**, 7014 (2000)

2) R. G. Hemker *et al, "*Dynamic Effects In Plasma Wakefield Excitation", Physical Review Special Topics – Accelerators and Beams **3**, 061301 (2000).

3) S. Lee *et al*, "Plasma-Wakefield Acceleration Of A Positron Beam", Physical Review E **64**, 045501(R) (2001).

4) E. S. Dodd *et al*, "Hosing And Sloshing Of Short-Pulse Gev-Class Wakefield Drivers", Physical Review Letters **88**, 125001 (2002).

5) S. Deng *et al*, "Plasma wakefield acceleration in self-ionized gas or plasmas", Physical Review E **68**, 047401 (2003).

6) R. Maeda *et al*, "Possibility of a multibunch plasma afterburner for linear colliders", Physical Review Special Topics – Accelerators and Beams **7**, 111301 (2004).

Papers in preparation – titles are tentative

1) P. Muggli *et al.*, "Halo Formation Around Positron Beam Core"
2) C. Barnes *et al.*, "Measuring Ultra-short Beams at SLAC"

Student Theses

1) Brent E. Blue, M.S. UCLA, "Hosing Instability of the Drive Electron Beam in the E-157 Plasma-Wakefield Acceleration Experiment at the Stanford Linear Accelerator" December 2000.

2) Seung Lee, Ph.D. USC, "Non-linear Plasma Wakefield Acceleration: Models and Experiments". May 2002.

3) Sho Wang, Ph.D. UCLA, "X-ray Synchrotron Radiation in a Plasma Wiggler" June 2002.

4) Brent E. Blue, Ph.D. UCLA, "Plasma Wakefield Acceleration of An Intense Positron Beam" January 2003

5) Wei Lu, M.S. UCLA, "Some Results on Linear and Nonlinear Plasma Wake Excitation : Theory and Simulation Verification"

6) Chenkun Huang, M.S. UCLA, "Development of a Novel PIC code for Studying Beam-Plasma Interactions"

7) Caolionn O'Connell, Ph.D. Stanford, "Field Ionization of Neutral Lithium Vapor using a 28.5 GeV Electron Beam"

8) Devon Johnson, Ph.D. UCLA, “Positron production in a plasma wakefield accelerator”
9) Chris Barnes, Ph.D. Stanford, “Phase space determination in the FFTB and investigation of hosing effects”
10) Suzhi Deng, Ph. D. USC, “Models and Physics of Plasma Wakefield Accelerators in Beam-ionized gases”

Student Theses in Preparation

1) Chengkun Huang, Ph.D. UCLA, “Quasi-static Particle-In-Cell modeling of Beam-Plasma Interactions”
2) Miaomiao Zhou, Ph.D. UCLA, “Accelerating ultra-short electron/positron bunches in field ionization produced plasmas”
3) Erdem Oz, Ph.D. USC, “Plasma Dark Current in Plasma Wake Field Accelerators (PWFA)”
4) Wei Lu, Ph. D. UCLA, “A theoretical formalism for wake excitation and acceleration in the blowout regime”

More than 15 invited presentations and/or papers at conferences, workshops, universities, and laboratories.

References

1 C. Joshi and T. Katsouleas, Plasma Accelerators at the Energy Frontier and on Tabletops, Physics Today, 47 (June 2003).

2 M. Tigner, Accelerator R&D. Eur. Phys. J. C 33, s01, s146–s148 (2004), http://dx.doi.org/10.1140/epjcd/s2003-03-017-5

3 Y. B. Fainberg et al., Wakefield excitation in plasma by a train of relativistic electron bunches. Fizika Plazmy vol. 20, pp. 674-681, 1994.

4 S. Lee et al., Phys. Rev. ST Accel. Beams 5, 011001 (2002)

5 P. Chen et al., *Phys. Rev. Lett.* **56**, 1252 (1986).

T. Katsouleas et al., *Phys. Rev A* **33**, 2056 (1986).

J. Rosenzweig et al., *Phys. Rev. Lett.* **61**, 98 (1998).

R. Ruth et al., *Particle Accelerators* **17**, 171 (1985).

6 C.L. O'Connell *et al*, "Plasma Production via Field Ionization", Physical Review Special Topics – Accelerators and Beams **9**, 101301 (2006)

7 R. Keinigs et al., *Phys. Fluids* **30**, 252 (1987).

8 R. Hemker et al., *Phys. Rev. STAB* **3**, 061301 (2000).

9 C. Huang et. al., Proceedings, 18th Annual Review of Progress in Computational Electromagnetics, P 557 (2002).

10 **LiTrack: A Fast longitudinal phase space tracking code with graphical user interface.** K.L.F. Bane, P. Emma (SLAC) . SLAC-PUB-11035, PAC-2005-FPAT091, Apr 2005. 3pp. Contributed to Particle Accelerator Conference (PAC 05), Knoxville, Tennessee, 16-20 May 2005. Published in *Knoxville 2005, Particle Accelerator Conference* 4266

11 P.B. Wilson, in: Proc. SLAC Summer Institute on Particle Physics, SLAC, July 1985, SLAC Report 296, January 1986, pp. 273–295. Also SLAC-PUB-3891, February 1986.

12 D. Whittum et al., *Phys. Rev. Lett.* **67**, 991 (1991).

13 E. Oz *et al.*, submitted to Phys. Rev. Lett. 2006

14 J. Seeman, W. Brunk, R. Early, M. Ross, E. Tillmann and D. Walz, SLC Energy Spectrum Monitor using Synchrotron Radiation. 1986 Linear Accelerator Conference Proceedings, SLAC-PUB-3945, June 1986.